Received: 9 October 2020 | Revised: 11 February 2021 | Accepted: 12 March 2021

DOI: 10.1002/ptr.7103

RESEARCH ARTICLE

WILEY

Usnic acid suppresses cervical cancer cell proliferation by inhibiting PD-L1 expression and enhancing T-lymphocyte tumor-killing activity

Tong Xin Sun | Ming Yue Li | Zhi Hong Zhang | Jing Ying Wang | Yue Xing | MyongHak Ri | Cheng Hua Jin | Guang Hua Xu | Lian Xun Piao | Hong Lan Jin | Hong Xiang Zuo | Juan Ma | Xuejun Jin

Molecular Medicine Research Center, College of Pharmacy, Yanbian University, Yanji, China

Correspondence
Juan Ma and Xuejun Jin, Molecular Medicine Research Center, College of Pharmacy, Yanbian University, Yanji 133002, Jilin, China.
Email: majuan@ybu.edu.cn (J. M.) and xjjin@ybu.edu.cn (X. J.)

Funding information
the 111 Project of the base of recruiting talents for disciplinary innovation on natural resources & functional molecules, Grant/Award Number: 111; the 13th five-year program of science and technology of the ministry of education of Jilin province, Grant/Award Number: JJKH20191152KJ; National Natural Science Foundation of China, Grant/Award Numbers: 81660608, 81760657

The programmed cell death 1 (PD-1)/programmed death ligand 1 (PD-L1) pathway is abnormally expressed in cervical cancer cells. Moreover, PD-1/PD-L1 blockade reduces the apoptosis and exhaustion of T cells and inhibits the development of malignant tumors. Usnic acid is a dibenzofuran compound originating from *Usnea diffracta* Vain and has anti-inflammatory, antifungal, and anticancer activities. However, the molecular mechanism of its antitumor effects has not been fully elucidated. In this work, we first observed that usnic acid decreased the expression of PD-L1 in HeLa cells and enhanced the cytotoxicity of co-cultured T cells toward tumor cells. Usnic acid inhibited PD-L1 protein synthesis by reducing STAT3 and RAS pathways cooperatively. It was subsequently shown that usnic acid induced MiT/TFE nuclear translocation through the suppression of mTOR signaling pathways, and promoted the biogenesis of lysosomes and the translocation of PD-L1 to the lysosomes for proteolysis. Furthermore, usnic acid inhibited cell proliferation, angiogenesis, migration, and invasion, respectively, by downregulating PD-L1, thereby inhibiting tumor growth. Taken together, our results show that usnic acid is an effective inhibitor of PD-L1 and our study provide novel insights into the mechanism of its anticancer targeted therapy.

KEYWORDS
antitumor activity, lysosome, PD-L1 inhibitor, T cells, Usnic acid

1 | INTRODUCTION

Cervical cancer is one of the most common types of gynecological malignancy and is caused by persistent infection with high-risk human papillomavirus (HPV) (Arbyn et al., 2020). More than 90% of cervical cancers are accompanied by high-risk HPV infections. Other risk factors can also induce cervical cancers such as multi-parity, tobacco, malnutrition, and poor genital hygiene (Kumar & Bhasker, 2013). Despite the advances in screening methods and preventive vaccines, cervical cancer still has the fourth highest incidence of cancer among women, ranking after breast, colorectal, and lung cancer (Lee

Abbreviations: Baf, Bafilomycin A1; CHX, cycloheximide; DAPI, diamidino-phenyl-indole; DMSO, dimethyl sulfoxide; ERK, extracellular signal-regulated kinase; GAPDH, glyceraldehyde-3-phosphate dehydrogenase; IFN-γ, interferon-γ; IP, immunoprecipitation; JAK, janus-like kinase; MEK, mitogen-activated protein kinase kinase; MG-132, benzyloxycarbonyl-Leu-Leu-L-leucinal.; MITF, microphthalmia-associated transcription factor; MMP-9, matrix metalloproteinase-9; mTOR, mammalian target of rapamycin; MTT, 3-(4,5-dimethylthiazol-2-yl)-2,5-diphenyl-tetrazolium bromide; p70S6K, ribosomal protein S6 kinase; PBS, phosphate buffered solution; PD-1, programmed cell death-1; PD-L1, programmed cell death ligand-1; RT-PCR, reverse transcription-polymerase chain reaction; SHP-2, SH2 domain-containing protein tyrosine phosphatase 2; siRNA, short interfering RNA; STAT3, signal transducers and activators of transcription-3; TFE3, translocation factor E3; TFEB, transcription factor EB; TNF-α, tumor necrosis factor-α; Topo-1, Topoisomerase-I; VEGF, vascular endothelial growth factor.

Tong Xin Sun and Ming Yue Li contributed equally to this study.

et al., 2020; Liontos, Kyriazoglou, Dimitriadis, Dimopoulos, & Bamias, 2019). Therefore, novel therapeutic targets and prognostic indicators to improve the survival rate of patients with cervical cancer are urgently required. However, the occurrence, development, and metastasis of malignant tumors are complex processes involving multiple genes and factors and are related to the immune functions of patients.

Previous studies have reported that the programmed cell death 1 (PD-1)/programmed death ligand 1 (PD-L1) pathway is abnormally expressed in cervical cancer cells, and HPV positivity was positively correlated with increased PD-L1 expression (Liu et al., 2019). PD-1 receptors on T cells specifically bind to PD-L1 ligands on tumor cells, thereby activating the PD-1/PD-L1 pathway and inhibiting the tumor-killing activity of T cells, and promoting the secretion of inflammatory cytokines (Juneja et al., 2017). Moreover, persistent inflammation can promote the development of malignant tumors (Li, Zhang, Wang, Zuo, & Jin, 2019). PD-1/PD-L1 blockade reduces the apoptosis and exhaustion of T cells and enhances the lethality of the immune system (Badoual et al., 2013). Thus, blocking the PD-L1/PD-1 signaling pathway is considered a valuable strategy in the treatment of cervical cancer.

Molecular targeted therapy, as a hotspot in the field of antitumor research, provides a new approach for the treatment of patients with advanced cervical cancer (Zammataro et al., 2019). Signal transducer and activator of transcription 3 (STAT3) is a transcription factor closely related to tumors (Baek et al., 2016). The STAT3 signaling pathway has an important role in the occurrence and development of tumors, and has been shown to be aberrantly-expressed and constitutively-activated in cervical cancer which increases as the lesion progresses (Shukla et al., 2010). STAT3 activation is mainly mediated through the JAK/Src/STAT3 signaling pathway (Chai et al., 2016), but it can also be activated by inflammatory cytokines such as tumor necrosis factor-α (TNF-α) (De Simone et al., 2015; Kim et al., 2020). STAT3 interacts with tyrosine residues in the receptor through the SH2 domain, and promotes STAT3 phosphorylation, thereby promoting its activation and translocation to the nucleus (Zhang, Kuang, Wang, Sun, & Gu, 2015). The persistent phosphorylation of STAT3 can promote PD-L1 expression and cause tumorigenesis (Tong et al., 2020).

Oncogenes of the RAS family (H-RAS, K-RAS, and N-RAS) are located on the cell membrane and are involved in the regulation of cell proliferation and differentiation (Aoki, Niihori, Narumi, Kure, & Matsubara, 2008). A small amount of activated P21 protein maintains normal cell differentiation. When the RAS oncogene is mutated, the RAS protein is activated, accelerating cell growth and proliferation, and ultimately leading to the malignant transformation of cells (Haigis et al., 2008). The activation of RAS further enables its binding to the amino terminus of the serine/threonine protein kinase RAF-1 to activate it. RAF-1 can phosphorylate MEK1/MEK2, whereupon MEK can selectively activate ERK1 and ERK2 (Drosten et al., 2010). Continuous activation of RAS protein can up-regulate the expression of PD-L1, causing abnormal cell proliferation and promoting tumor formation (Coelho et al., 2017). Activated (oncogenic) RAS can also induce a malignant phenotype in human cervical cells and contribute to cancer development and augments cell growth in vitro and tumorigenicity in vivo (Mora, Rosales, & Rosales, 2007).

In Chinese medicine, *Usnea diffracta* Vain was often used to treat cancer, tuberculosis, asthma and so on and was recorded in Chinese classical anti-cancer plant books such as *Kang Ai Zhi Wu Yao Ji Qi Yan Fang* and *Kang Ai Zhong Yao* (Chang, 1998; Cheng & Li, 1998). Usnic acid is a dibenzofuran compound originating from a traditional medicine *Usnea diffracta* Vain (Ingólfsdóttir, 2002). In addition, usnic acid is widely used in medicine because of its antibacterial, antiviral, and anticancer biological activities (Kim et al., 2018; Luzina & Salakhutdinov, 2018). However, the molecular mechanism of the antitumor effects of usnic acid has not been fully elucidated. Therefore, the current study aimed to investigate the effectiveness of usnic acid as a treatment for cancer and to identify the underlying mechanisms of its anticancer activity.

In the present study, we confirmed the antitumor ability of usnic acid. We found that usnic acid inhibited PD-L1 expression and enhanced the activity and killing capacity of T cells. Moreover, usnic acid was further demonstrated be a potential valuable novel therapy for human cervical cancer.

2 | MATERIALS AND METHODS

2.1 | Cell culture and reagents

The human colorectal cancer HCT-116, human lung cancer A549, human cervical cancer (HeLa, SiHa, and CaSKi), normal human cervical epithelial cell line HcerEpic and human liver cancer Hep3B cells were obtained from American Type Culture Collection (ATCC, Manassas, VA, USA). HCT-116 Cells were maintained in Roswell Park Memorial Institute (RPMI) supplemented with 1% penicillin–streptomycin (Invitrogen, Carlsbad, CA, USA) and 10% heat-inactivated fetal bovine serum (FBS, Gibco, Grand Island, NY, USA). HeLa, SiHa, CaSKi, HcerEpic, Hep3B, A549, and HUVEC cells were grown in DMEM medium supplemented as above. All cells were cultivated in a humidified incubator including a 5% CO_2 atmosphere at 37°C. After reaching confluence, cells were separated with trypsin/ethylene diamine tetraacetic acid (EDTA) for passage. Tumor necrosis factor alpha (TNF-α) was provided by R&D Systems (Minneapolis, MN, USA). Dimethyl sulfoxide (DMSO), MG-132, cycloheximide (CHX), and Bafilomycin A1 (Baf) were purchased from Sigma Chemical Co. (St. Louis, MO, USA). The probes LysoTracker was obtained from Invitrogen (Carlsbad, CA, USA). Usnic acid was dissolved in dimethyl sulfoxide (DMSO) to a stock concentration of 100 mM and stored at −20°C in the dark before utilization. Usnic acid was purchased from Chengdu Herbpurify CO., LTD (Chengdu, China) and the structure of it is shown in Figure 1a. The purity of usnic acid was over 98% in HPLC analysis.

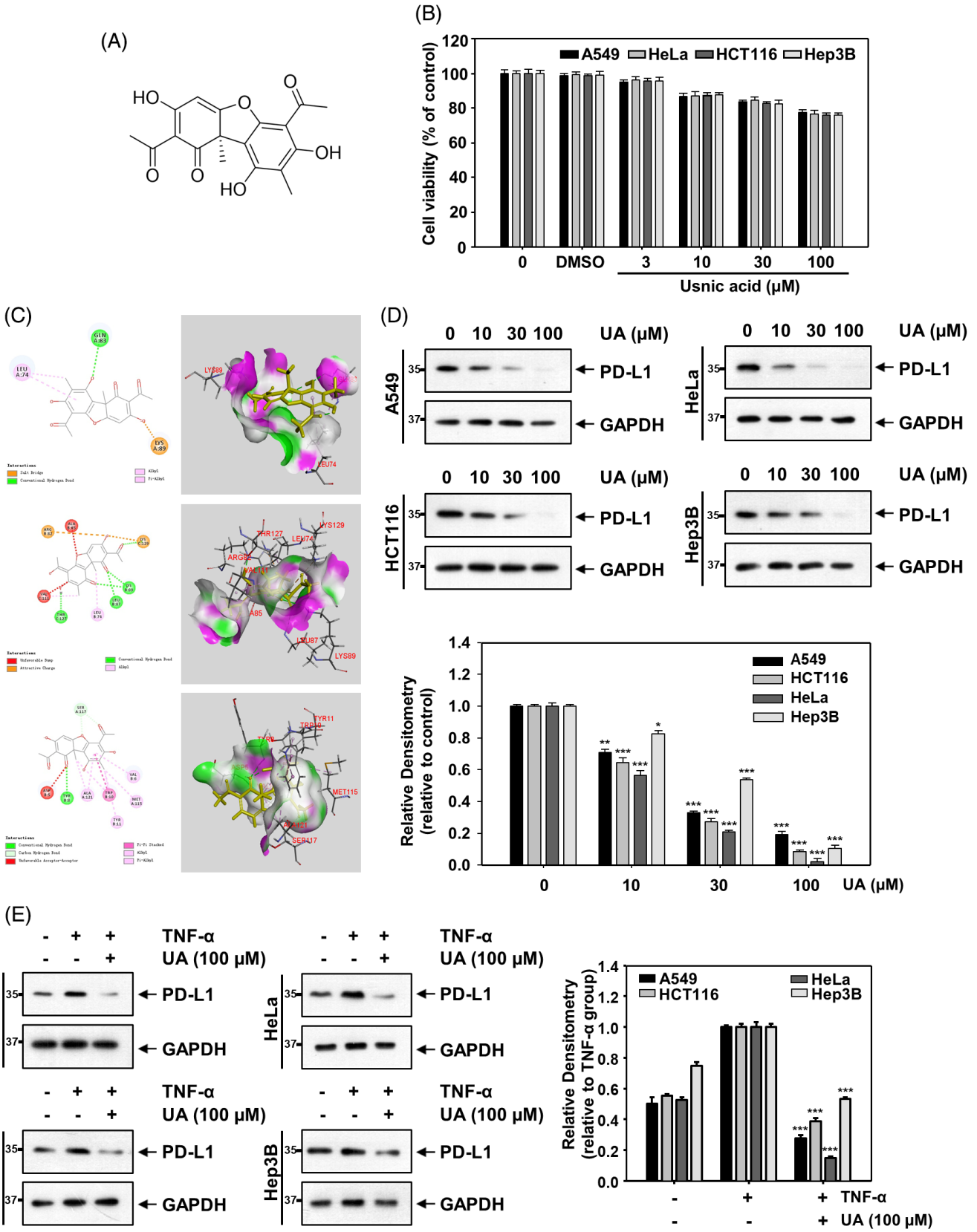

FIGURE 1 Effect of usnic acid on the expression of PD-L1 protein in various cancer cell lines. (a) Chemical structure of usnic acid. (b) HeLa, A549, HCT116, and Hep3B cells were treated with the indicated concentrations of usnic acid and were determined the relative cell viability by MTT assays after 24 h. (c) Usnic acid was bound with the binding domain in PD-L1 (upper, PDB ID: 5C3T; middle, PDB ID: 5O5Y; lower, PDB ID: 5O45). Binding mode was shown in 2D (left) and 3D (right). The ligand is shown in yellow. (d) HCT116, A549, HeLa, and Hep3B cells were treated with indicated concentration of usnic acid for 12 h, and cell lysates for PD-L1 were analyzed by western blotting. (e) Cells were incubated under 10 ng/mL TNF-α in the absence or presence of 100 μM usnic acid for 12 h, PD-L1 expressions were detected by western blotting. All data are presented as the mean ± SD of three independent experiments and representative data are shown. $^{*}p < 0.05$, $^{**}p < 0.01$, $^{***}p < 0.001$ [Colour figure can be viewed at wileyonlinelibrary.com]

2.2 | Cell viability assay

The relative cell viability was performed using the thiazolyl blue tetrazolium bromide (MTT) assay (Sigma-Aldrich). HCT-116, HeLa, HcerEpic, A549, and Hep3B cells were seeded in 96-well plates at a density of 4×10^3 cells/well. After 12 h, the cells in each well adhered to the wall and were incubated with DMSO and 3, 10, 30, and 100 μM concentrations of usnic acid. After 24 h incubation, 10 μL of MTT was added to each well at 37°C, 5% CO_2 atmosphere for 4 h. Then, 100 μL DMSO was added to dissolve the formazan. The absorbance values at 570 nm were determined with Multiskan GO (Thermo Electron Corp., Marietta, OH, USA), which can indirectly reflect the number of living cells.

2.3 | Homology modeling and molecular docking

The molecular docking simulations were carried out using Discovery Studio 2017/CDOCKER protocol (Accelrys, San Diego, USA) to explore the binding modes between the structure of usnic acid with the proteins of PD-L1, STAT3, and RAS. The structures of PD-L1 (PDB IDs: 5C3T, 5O5Y, and 5O45), STAT3 (PDB IDs: 3CWG, 4E68, 4ZIA, and 5U5S), and RAS (PDB IDs: 4EFL, 3X1W, and 2CL7) were deposited in protein databank respectively. By using the ligand preparation and minimization model, the spatial binding pattern between usnic acid and PD-L1/STAT3/RAS LBD was investigated in Discovery Studio 2017.

2.4 | Western blotting analysis

After cold PBS washing, cells were lysed in ice-cold lysis buffer (50 mM Tris–HCl, pH 7.5, 1% NP-40, 1 mM EDTA, 1 mM phenylmethyl sulfonylfluoride) supplemented with proteinase and phosphatase inhibitor cocktail (BD Biosciences, San Diego, CA, USA). Thirty micrograms of nuclear extract or fifty micrograms of whole-cell extracts protein samples were separated by 6–12% SDS-polyacrylamide gels and transferred to a polyvinylidene difluoride membrane (PVDF) (Millipore, Bedford, MA, USA). After being blocked with 5% skim milk, membranes were incubated with primary antibodies overnight at 4°C and incubation with an appropriate secondary antibody (1:2000) conjugated to horseradish peroxidase. Then, protein bands were visualized by enhanced chemiluminescence according to the instructions of the manufacturer (Amersham Pharmacia Biotec, Buckinghamshire, UK). Antibodies (1:500 dilution) for STAT3 (sc-482), mTOR (sc-8319), MEK (sc-81504), p70S6K (sc-8418), ERK1/2 (sc-514302), Topo-I (sc-5342), VEGF (sc-152), GAPDH (sc-365062), and MMP-9 (sc-393859) were obtained from Santa Cruz Biotechnology. Antibodies (1:1000 dilution) for pTyr705 STAT3 (9145), SHP-2(3397), c-RAF (9422), p-c-RAF (9427), pSer727 STAT3 (9134), p-MEK (9121), p-JAK1 (3331), TFEB (37785), p-JAK2 (3776), TFE3 (14779), p-Src (6943), MITF (12590), p-mTOR (2971), p-p70S6K (9204), Cyclin-D1 (2922), phospho-ERK1/2 (4370), c-Myc (9402), and Src (21093) were purchased from Cell Signaling Technology. Antibodies (1:1000 dilution) for PD-L1 (NBP1-76769), JAK1 (NB100-82005), and JAK2 (NBP2-67429) were purchased from novus Biologicals. Antibody (1:5000 dilution) for RAS (ab108602) was purchased from abcam. Antibody (1:5000 dilution) for HA-tag (M20003) was purchased from abmart. Antibody (1:2000 dilution) for Flag-tag (F-2922) was purchased from sigma. Then, protein bands were visualized by enhanced chemiluminescence according to the instructions of the manufacturer (Amersham Pharmacia Biotec, Buckinghamshire, UK).

2.5 | Reverse transcription-PCR (RT-PCR) analysis

HeLa cells were cultured in 6 cm culture plates to clustering. Then, the cells were incubated with different concentrations of usnic acid (10, 30, and 100 μM) with or without 10 ng/mL TNF-α. Total RNA from HeLa cells was extracted by Trizol reagent (Invitrogen) and RNA Mini kit (Qiagen, Valencia, CA, USA). Total RNA (2 μg) was reverse-transcribed using the RT-PCR kit (Invitrogen) according to the manufacturer's instructions. The spatial structure of RNA was destroyed by incubation at 65°C for 10 min. Next, the extension was performed at 55°C for 30 min, and the reverse transcription of RNA to cDNA by incubation at 85°C for 5 min. Then PCR amplification is performed. The cycling conditions were 94°C for 4 min followed by 35 cycles of 94°C for 30 s, 58°C for 30 s, and 72°C for 30 s, and a final extension stage of 72°C for 5 min. The PCR products on 3% agarose gels were labeled with ethidium bromide, and then stained bands were observed under UV light. Quantification was calculated using the $2^{-\Delta\Delta CT}$ method and was presented as fold change. The expression of each target gene was normalized to GAPDH mRNA and the primers of it were (forward and reverse, 5′-3′): ACCACAGTCCATGCCATCAC (sense) and TCCACCCCCTGTTGCTGTA (antisense). The primer P118295 F (5′-TGCCGACTACAAGCGAATTAC-3′) is picked from the exon 3 (bases 308…328) of PD-L1 gene (gene number 29126) transcript variant 1, and the primer P118295 R (5′-CTGCTTGTCCAG ATGACTTCG-3′) is picked from the exon 4 (complementary to bases 95…115).

2.6 | Transfections of the plasmids and small interfering RNA (siRNA)

According to the manufacturer's instructions, transfections were carried out in HeLa cells grown to 60% confluency in 6 cm dishes using Lipofectamine 2000 reagent (Invitrogen) and the designated siRNA or overexpressed plasmid. Then, the transfected cells were cultured for 48 h. PD-L1 (*CD274*) siRNA (5′-CAGCAUUGGAACUUCUGAU-3′), SHP-2 (*PTPN11*) siRNA (5′-UGACAUCGCGGAGAUGGUU-3′), RAS siRNA (5′-GGACUUAGCAAGAAGUUAUTT-3′), and they paired control siRNAs were obtained from Bioneer (Daejeon, Korea). STAT3 siRNA (5′-GCAGUUUCUUCAGAGCAGGUAUCUU-3′) and control siRNA were provided by Santa Cruz (CA, USA). Briefly, the CD274, STAT3, or RAS gene coding sequences (CDS) were constructed on the

overexpression plasmid vectors, respectively, the transcript number of CD274 was NM_014143 (GV362 vector, XhoI/BamHI restriction enzymes), STAT3 was NM_139276 (GV141 vector, XhoI/KpnI restriction enzymes), RAS was NM_033360 (GV141 vector, XhoI/EcoRI restriction enzymes). The overexpression plasmids of RAS, PD-L1, STAT3, and paired control plasmids were obtained from Shanghai Genechem (Shanghai, China). HA-Ub (M. Jung, Georgetown University) and control vector were synthesized in our laboratory.

2.7 | Immunofluorescence assay

HeLa cells were seeded at approximately 1×10^4 cells/well confluence in 24-well chamber slides. After 24 h, cells were treated with usnic acid (100 μM) and incubated for 12 h with or without 10 ng/mL TNF-α. Cells treated with DMSO and under with or without TNF-α conditions were used as negative and positive controls, respectively. After treatment, removal of each wells' culture medium, the chamber slides were washed twice with preheating of PBS, fixed with fresh 4% formaldehyde for 30 min, and washed three times with PBS at room temperature. Cells were then permeabilized with 0.2% Triton X-100 and blocked in 5% BSA in PBS for 30 min at room temperature and incubated overnight with the RAS (Abcam; cat. no. ab108602; 1:100 dilution), PD-L1 (Novus Biologicals; cat. no. NBP1-76769; 1:50 dilution), pTyr705 STAT3 (Cell Signaling Technology; cat. no. 9145; 1:100 dilution), or STAT3 (Santa Cruz Biotechnology; cat. no. sc-482; 1:50 dilution) antibody at 4°C. After being rinsed three times in PBS, the cells were incubated with secondary antibodies, such as Alexa flour 488 goat anti-rabbit or Alexa flour 568 goat anti-mouse for 30 min at room temperature. After being stained with DAPI (4′,6-diamidino-2-phenylindole), the glass slide was removed from 24-well and sealed by glycerin. After 24 h, cells were examined with confocal laser scanning microscopy (Nikon, Japan).

2.8 | Immunoprecipitation

After being transfected with designated overexpressed plasmids, HeLa cells were cultured in 6-cm Petri dishes for 12 h after treated with usnic acid (100 μM) and with or without 10 ng/mL TNF-α. Whole-cell extracts were lysed in IP buffer (containing 1% Nonidet P-40, 50 mM EDTA, 150 mM NaCl, 50 mM Tris–HCl, pH 7.4 and protease inhibitors cocktail). Each immunoprecipitation analyzed 1 mg protein lysates. To bind the antigen, the primary antibody of RAS (Abcam; cat. no. ab108602; 1:100 dilution), STAT3 (Santa Cruz Biotechnology; cat. no. sc-482; 1:500 dilution), HA-tag (Abmart; cat. no. M20003; 1:100 dilution), or Flag-tag (Abmart; cat. no. M20008; 1:100 dilution) was added to the lysates and followed by rotation at 4°C overnight. Then, 30 μL of protein A/G PLUS agarose beads (Santa Cruz) were added and incubation continued. After 1 h of incubation, beads were washed 3 times with cold IP buffer and add SDS-PAGE sample buffer, then the sample was boiled at 100°C for 5 min, subsequently detected by western blotting.

2.9 | LysoTracker red staining

To label lysosomes, HeLa cells were incubated with LysoTracker Red DND-99 dye (75 nM) (Invitrogen, L-7528) for 30 min at 37°C. The medium was aspirated and washed twice with pre-warmed PBS to remove the unbound dye. Red fluorescence can be observed by confocal laser scanning microscopy.

2.10 | Cell surface staining and flow cytometry analysis

Cells were collected after treated with DMSO, 100 μM usnic acid, or PD-L1 siRNA transfection. After being washed with phosphate-buffered saline (PBS), cells (1×10^6 cells/mL) were incubated with anti-PD-L1 antibody (Novus Biologicals; cat. no. NBP1-76769; 1:200 dilution) for 1 h on ice in dark. Then cells were incubated with the FITC-conjugated secondary antibody rabbit. Cells surface staining was quantitatively analyzed by Accuri C6 flow cytometry.

2.11 | Cervical cancer cells/T-cell co-culture model and T-cell killing assay

Participants provided written informed consent and the program was confirmed by the Medical Ethics Committee of Yanbian University. CD3+ T lymphocytes were purified from the blood of healthy human donors using Lymphoprep density-gradient centrifugation. Briefly, cervical cancer (HeLa, SiHa, CaSKi) cells were plated at 5×10^4/well in 24-well plates and activated by incubation with anti-CD28, anti-CD2, anti-CD3 antibody (100 ng/mL), and IL-2 (10 ng/mL). After being pretreated with usnic acid (100 μM) for 12 h or PD-L1 siRNA transfection for 48 h, activated T cells were incubated with cervical cancer cells at a ratio of 10:1. After 48 h, cytotoxicity assay was conducted using colony formation assay (crystal violet staining) and lactate Journal Pre-proof dehydrogenase (LDH) release assay (Mlbio, Shanghai, China). The contents of TNF-α and IFN-γ in media were measured using cytokine ELISA (Mlbio, Shanghai, China).

2.12 | Colony formation assay

Treated HeLa cells were cultured in DMEM containing 10% FBS and seeded in 6-well culture plates for colony formation assay. Each of the wells was maintained at 37°C in a 5% CO_2 atmosphere for 15–25 days, and the medium was replaced with fresh media every 7 days. After 20 days, colonies could be obviously visible and were washed twice with PBS to remove media. Then, the survived tumor cells were fixed with 10% formaldehyde for 5 min and stained with 1% crystal violet for 30 s at ambient temperature. After being washed with PBS and air-dried, the colonies were counted.

2.13 | EdU labeling and immunofluorescence

Treated HeLa cells were seeded in 96-well culture plates at 37°C in a 5% CO_2 atmosphere for 24 h. Then, each of the wells was cultured with 50 μmol/L of EdU (Ribobio, Guangzhou, China) for 2 h. After being fixed for 30 min, the cells were exposed to 100 μL of 1 × Apollo reaction cocktail for 30 min. Whereafter, Hoechst 33342 was added to each well to stain the cell nuclei. The stained cells were observed with Olympus IX83 inverted fluorescence microscope.

2.14 | Tube formation assays

The ability of treated HUVEC cells to form network structures was tested on a matrigel basement membrane matrix. First, 300 μL matrigel was dispensed onto 96-well plates and solidified for 1 h at 37°C. HUVEC cells were suspended in DMEM medium containing 10% FBS and were seeded into each well. After 4 h of incubation at 37°C in a 5% CO_2 atmosphere, cells tube-like structures and numbers were photographed using a microscope.

2.15 | Scratch assay

Scratch assays were applied to determine treated HUVEC cell migration efficiency. Treated HUVEC cells were seeded on 24-well plates and were cultured with DMEM medium containing 10% FBS to obtain a full confluent monolayer. After 24 h, the cells reached 80% confluence, then, the cells were scratched with a pipette tip to create a straight cell-free "scratch" on the well plate to form a wound. Subsequently, each well was washed with PBS to remove debris and incubated with different treatments. The migration rates of cells in the "scratch" were photographed using a microscope at identical locations and analyzed by comparing final gap widths to initial gap widths.

2.16 | Matrigel transwell invasion assay

The invasion assay was performed using the Transwell system Boyden chamber (Costar, MA, USA). Treated HUVEC cells were suspended in serum-free DMEM medium and were added to the upper wells of the chambers. Then, 600 μL of the DMEM medium supplemented with 10% FBS was added to the lower chamber. After treatment for 24 h at 37°C in a 5% CO_2 atmosphere, the non-migrated cells were wiped off from the top of the upper wells using cotton swabs. Successfully migrated cells were fixed with 4% paraformaldehyde and stained with 0.1% crystal violet. Thereafter, invaded cells were photographed by a fluorescence microscope.

2.17 | Statistical analysis

All values are expressed as mean ± standard deviation (SD) of the mean of n = 3 experiments. Comparisons of the results were carried out using one-way ANOVA and Tukey's multiple comparison tests (Graphpad Software, Inc, San Diego, CA, USA). Statistical significance was defined as $p < 0.05$.

3 | RESULTS

3.1 | Identification of usnic acid as an inhibitor of PD-L1 expression in various cancer cell lines

Increased expression of PD-L1 leads to suppression of the cytotoxic activity of T cells, thus promoting immune evasion of tumor cells (Wang, Wang, Yao, Li, & Xu, 2018). Based on this, this part investigated whether usnic acid affects PD-L1 expression. First, to evaluate the effect of usnic acid on the viability of cancer cells, MTT assays were performed. Usnic acid did not display significant cellular toxicity on various cancer cell lines up to 100 μM; moreover, DMSO treatment has no effect on cell viability in cells (Figure 1b). And, usnic acid was found to induce little cytotoxicity toward normal cervical cell line HcerEpic (Supplementary Figure 1A). To understand the structural basis of the inhibitory effects, the binding mode of usnic acid and PD-L1 was investigated. Molecular docking assays showed that usnic acid had a high-affinity interaction with protein 5C3T (binding pockets consisting of Lys89, Gln83, and Leu74), protein 5O5Y (binding pockets consisting of Arg82, Thr127, Leu74, Lys129, Val111, A85, Leu87, and Lys89) and protein 5O45 (binding pockets consisting of Tyr11, Trp10, Tyr8, Asp5, Val6, Met115, Ala121, and Ser117) of PD-L1 (Figure 1c). Next, to address whether the inhibition of PD-L1 by usnic acid is cell line-specific, these studies were extended to a diverse set of tumor cell lines from tissues of various origins, including human colorectal cancer HCT-116, human cervical cancer HeLa, human lung cancer A549, and human liver cancer Hep3B cell lines. Because tumor necrosis factor-α (TNF-α) is a key inducer of PD-L1 expression, which promotes tumor growth by inducing cell survival, proliferation, angiogenesis, and epithelial-to-mesenchymal transition (Ju, Zhang, Zhou, Chen, & Wang, 2020). Therefore, 10 ng/mL of TNF-α was used to induce the expression of PD-L1, and there are no toxic effects in the treated cells at this concentration (Supplementary Figure 1B). As displayed in Figure 1d,e, the level of PD-L1 protein was dose-dependently restrained by usnic acid in all cell lines experimented with or without TNF-α. Together, these data suggest usnic acid reduces PD-L1 expression with few cytotoxic effects. The inhibition of PD-L1 protein in HeLa cells was most significant with usnic acid treatment. Therefore, HeLa cells were used for the subsequent experiments described in this study.

3.2 | Usnic acid inhibits the protein synthesis of PD-L1 and enhances its degradation

The next experiment investigated the mechanisms of PD-L1 down-regulation by usnic acid. First, this part examined whether usnic acid affects PD-L1 expression at the mRNA level. Reverse transcription-PCR (RT-PCR) assay revealed that usnic acid inhibited PD-L1 (*CD274*)

mRNA level in a dose-dependent manner in HeLa cells in the presence or absence of TNF-α-induced (Figure 2a). This indicated that usnic acid inhibits the transcription of PD-L1. Thereafter, to investigate the translational regulation of PD-L1 protein synthesis by usnic acid, the proteasome inhibitor MG-132 was used to prevent PD-L1 degradation. The synthesis rate of the PD-L1 protein was reflected by the accumulation rate of proteasomal inhibition. As shown in Figure 2b, PD-L1 protein in TNF-α-stimulated cells rapidly accumulated in the presence of MG132 (compare lane 2 with lane 4 in Figure 2b). In contrast, usnic acid inhibited PD-L1 protein accumulation even under cotreatment with MG-132 (see lanes 3 and 5 in Figure 2b). These results indicated that PD-L1 protein synthesis in HeLa cells is obviously inhibited in the presence of usnic acid. To investigate the effect of usnic acid on PD-L1 protein stability, HeLa cells were exposed to the protein translation inhibitor cycloheximide (CHX) to prevent de novo PD-L1 protein synthesis. With the increase in CHX treatment time, the PD-L1 protein levels of usnic acid-treated cells were lower than untreated cells under TNF-α stimulation (Figure 2c,d). Western blotting analysis revealed that overexpression of PD-L1 increased the levels of PD-L1, whereas treatment with PCMV had a minimal effect (Supplementary Figure 1C right). Moreover, usnic acid did not catalyze the ubiquitination of PD-L1 (Supplementary Figure 1C left). These

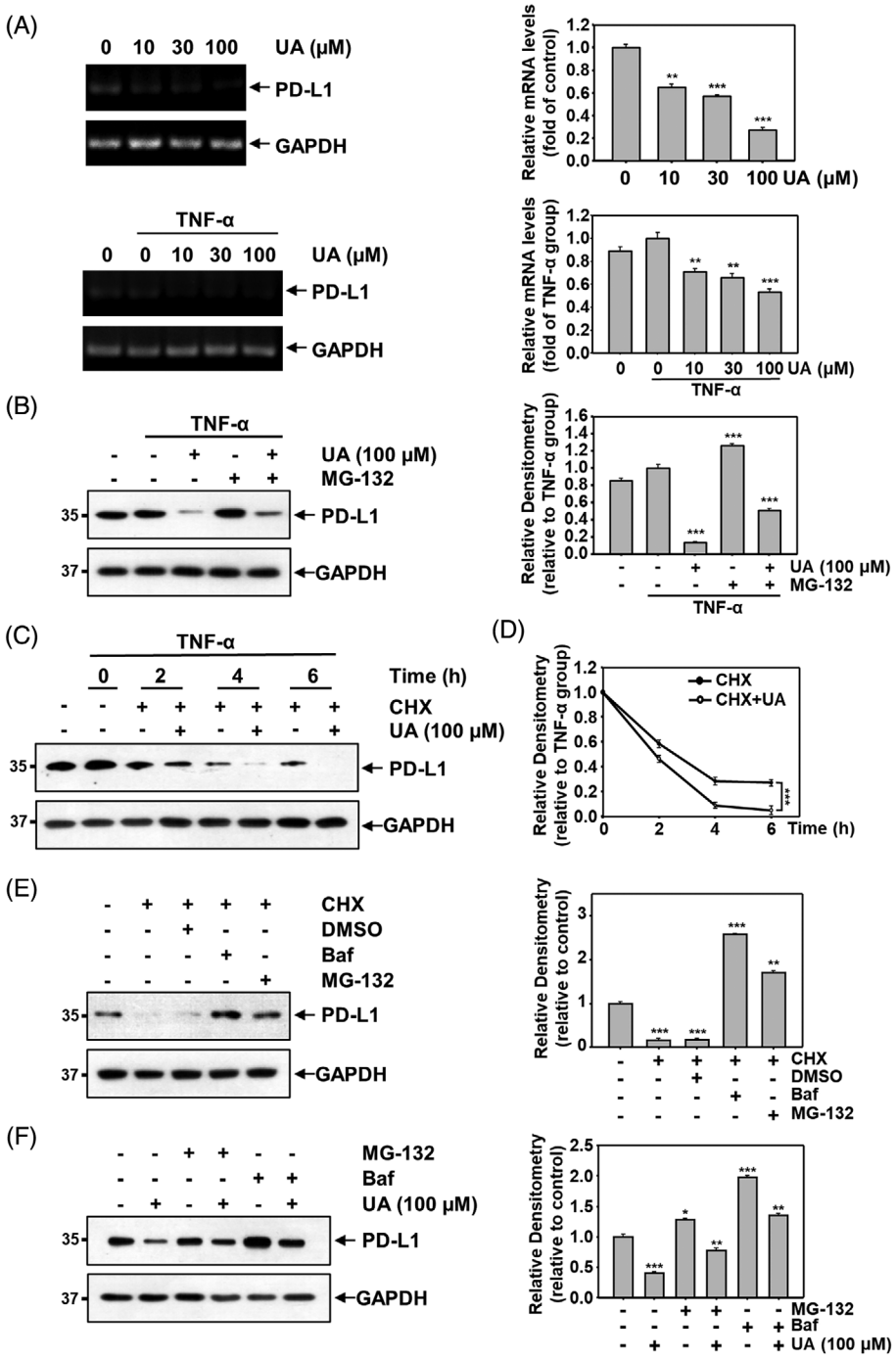

FIGURE 2 Effect of usnic acid on PD-L1 protein synthesis and degradation. (a) With or without TNF-α-stimulated, the quantitative RT-PCR analysis of PD-L1 mRNA level in HeLa cells treated with usnic acid (10 μM, 30 μM, 100 μM, 12 h). (b) HeLa cells were treated with MG-132 (10 μM) for 30 min before adding usnic acid (100 μM) and then the cells were incubated in TNF-α-stimulated for 6 h. The expression of PD-L1 in HeLa cells was under usnic acid treatment determined by western blotting. (c) HeLa cells were incubated in the presence of TNF-α-stimulated for 6 h. Western blotting analysis of the PD-L1 expression in HeLa cells was treated with usnic acid (100 μM) for the indicated time points in the presence of CHX (10 μM). (d) Quantification of PD-L1 intensity in (c). (e) Expression of PD-L1 determined by western blotting in HeLa cells treated with Bafilomycin or MG-132 in the presence of CHX for 6 h. (f) Western blotting measuring the PD-L1 expression in HeLa cells pre-treated with Baf or MG132, followed with or without usnic acid (100 μM) treatment for 6 h. All data are presented as the mean ± SD of three independent experiments and representative data are shown. $^{*}p < 0.05$, $^{**}p < 0.01$, $^{***}p < 0.001$

findings suggest that usnic acid inhibits the protein synthesis of PD-L1 and enhances its degradation.

3.3 | Usnic acid increases the biogenesis of lysosomes and promotes the translocation of PD-L1 to lysosomes, which accelerates the degradation of PD-L1

This part has discussed the mechanism of usnic acid promoting the degradation of PD-L1. There are two main pathways of protein degradation: the proteasome pathway and the lysosomal pathway (Sandri, 2016). Under CHX treatment, HeLa cells were incubated with proteasome inhibitor MG-132 or lysosomal inhibitor bafilomycin. As shown in Figure 2e, the degradation of PD-L1 was downregulated by MG-132 or bafilomycin. However, after HeLa cells were co-treated with usnic acid and MG-132 or bafilomycin, PD-L1 degradation was decreased more by bafilomycin then by MG-132 (Figure 2f). To determine whether usnic acid affected lysosomal function, lysosomes were stained with LysoTracker Red. Immunofluorescence assay indicated that the expression of lysosomes was obviously increased under usnic acid treatment (Supplementary Figure 2A). A study revealed that PD-L1 is targeted for lysosome compartment degradation (Burr et al., 2017). Immunofluorescence assays were further performed to investigate whether usnic acid promotes the translocation of PD-L1 to lysosomes. The results indicated that usnic acid increased the colocalization of PD-L1 and LysoTracker Red in HeLa cells (Supplementary Figure 2B), demonstrating the role of usnic acid in mediating lysosomal translocation of PD-L1.

The MiT/TFE proteins (including TFEB, TFE3, MITF) augment the lysosomal compartment, which triggers the biogenesis of lysosomes and promotes protein degradation (Li, Zhu, Xiang, Qiu, & Lin, 2020; Perera & Zoncu, 2016). We next investigated whether usnic acid induces the biogenesis of lysosomes dependent on the role of TFEB, TFE3, and MITF. Western blotting revealed that usnic acid treatment induced an increase in TFEB, MITF, and TFE3 in the nuclear fraction (Supplementary Figure 2C). Because mTOR signaling pathway activation inhibited MiT/TFE nuclear translocation (Li et al., 2016), the potential role of mTOR pathway was examined in modulating usnic acid-mediated TFEB, TFE3, and MITF nuclear translocation. As shown in Supplementary Figure 2D, usnic acid potently suppressed the phosphorylation of mTOR and p-70S6k in a concentration-dependent manner. Taken together, these data suggest that usnic acid induces MiT/TFE nuclear translocation through the suppression of mTOR signaling, and promotes PD-L1 degradation in lysosomes.

3.4 | Usnic acid inhibits PD-L1 expression on the cell surface and enhances T-lymphocyte tumor-killing activity

To examine whether usnic acid affects the surface expression levels of PD-L1, flow cytometry was performed. Western blotting analysis showed that silencing PD-L1 reduced the levels of PD-L1 (Supplementary Figure 3A), whereas treatment with control siRNA had a minimal effect. As shown in Figure 3a, usnic acid distinctly decreased the surface expression of PD-L1 on HeLa cells, similar to that caused by silencing of PD-L1 (*CD274*), indicating usnic acid could also decrease PD-L1 transportation to the plasma membrane. Cancer cells exploit PD-L1 to bind to PD-1 expressed by T cells and disrupt its immune surveillance, inducing the exhaustion of T cells (Juneja et al., 2017). To evaluate whether usnic acid could increase T cell activity in a co-culture model of HeLa cells and activated T cells, pure CD3+ T lymphocytes were isolated from total peripheral blood donated by healthy volunteers (Figure 3b). LDH release assay showed that usnic acid obviously enhanced the cytotoxicity of co-cultured T cells, and increased TNF-α and IFN-γ cytokines levels related to T cell killing activity in the medium compared with mono-cultured T cells (Figure 3d–f). These results were similar to the increased T cell-mediated cell killing by *CD274* silencing. Furthermore, this result was further confirmed by staining the surviving tumor cells with crystal violet (Figure 3c). Subsequently, the other two cervical cancer cell lines (SiHa and CaSKi cells) were used to further explore the effect of usnic acid on T cell activity. Similarly, usnic acid enhanced the cytotoxicity of co-cultured T cells and increased TNF-α and IFN-γ cytokines levels (Supplementary Figure 4). Collectively, these results indicate that usnic acid enhances the cytotoxicity of T cells by down-regulating PD-L1 surface expression.

3.5 | Usnic acid inhibits proliferation by decreasing PD-L1 in human cervical cancer cells

The effect of usnic acid on HeLa cell proliferation through PD-L1 was further investigated. Western blotting assay indicated that the expression of cell cycle regulatory proteins, including c-Myc and cyclin-D1 (Ma et al., 2016), was decreased by silencing of *CD274*, which was enhanced by co-treatment with usnic acid (Figure 4a). Furthermore, the expression of c-Myc and cyclin-D1 was promoted by overexpression of PD-L1, but usnic acid treatment limited this increase (Figure 4b). Moreover, the effect of usnic acid on cell proliferation was investigated by colony formation assays. As shown in Figure 4c and Supplementary Figure 3B, the clonogenic-forming ability of HeLa cells was greatly reduced by silencing of *CD274* or co-treatment with usnic acid. Overexpression of PD-L1 induced cell proliferation; however, co-treatment with usnic acid restrained this expression. These results were further confirmed using EdU incorporation assays whereby: usnic acid suppressed the number of EdU positive cells induced by PD-L1 (Figure 4d). Taken together, these results indicated that usnic acid inhibits proliferation by decreasing PD-L1 expression in human cervical cancer cells.

3.6 | Usnic acid inhibits angiogenesis, migration, and invasion by decreasing PD-L1 in endothelial cells

To investigate whether usnic acid affects angiogenesis in endothelial cells through PD-L1, *CD274* expression was silenced or

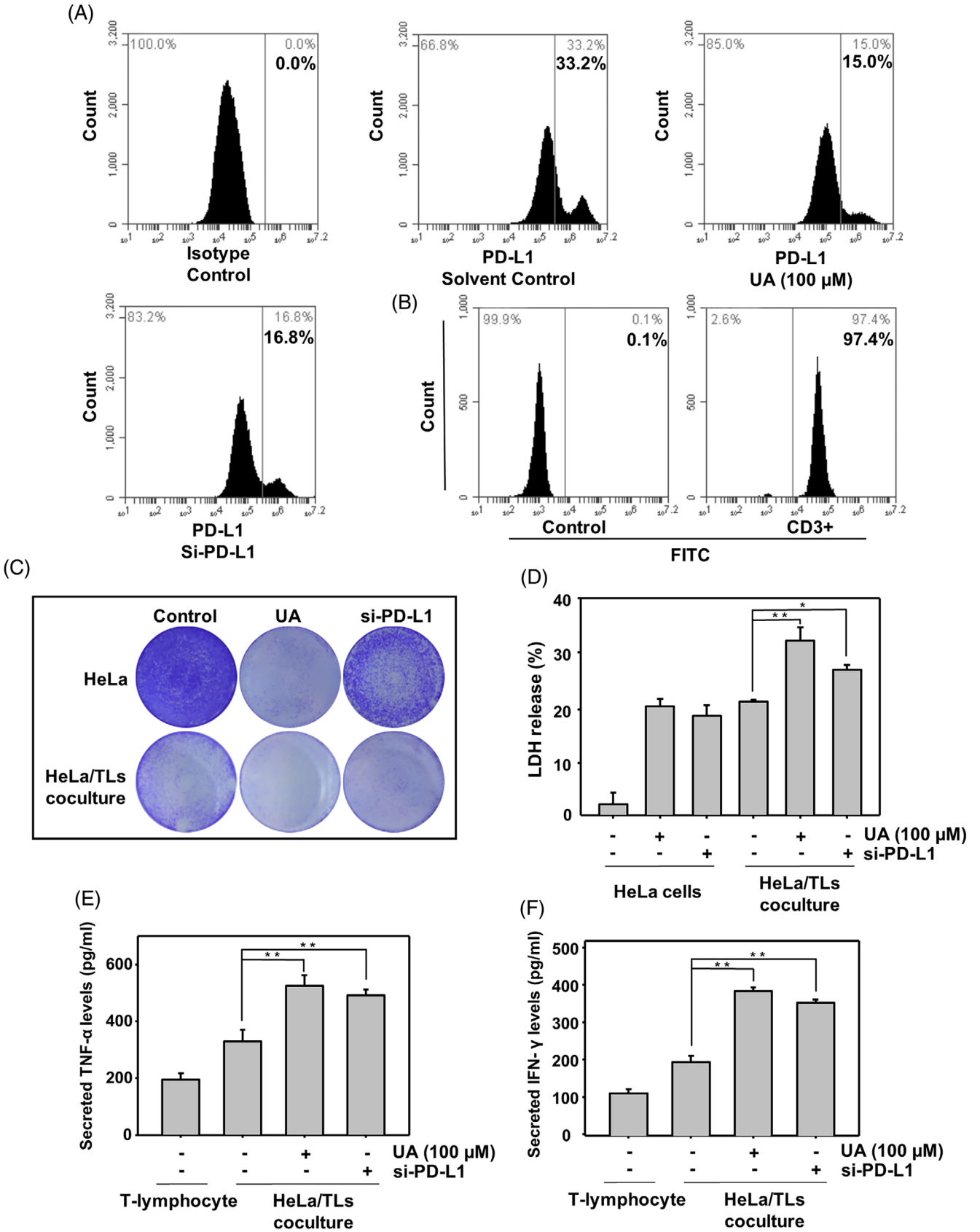

FIGURE 3 Effect of usnic acid on T-lymphocytes function and PD-L1 expression on the cell surface. (a) HeLa cells were incubated with DMSO, 100 μM usnic acid for 12 h or PD-L1 siRNA transfection for 48 h respectively. The levels of PD-L1 expression on the cell surface were detected by flow cytometry. (b) Human T-lymphocytes labeled with anti-human CD3 antibodies were analyzed by Flow cytometry assay. (d) HeLa cells were pretreated with or without 100 μM usnic acid for 12 h or PD-L1 siRNA transfection for 48 h, then were co-cultured with activated human T cells at a ratio of 1:10 for 48 h. The cytotoxicity of T cells was determined by LDH releasing assay. After 48 h coculture, surviving tumor cells were stained by colony formation assay (c). TNF-α and IFN-γ cytokines in the coculture medium were determined by ELISA (e and f). All data are presented as the mean ± SD of three independent experiments and representative data are shown. $^{*}p < 0.05$, $^{**}p < 0.01$, $^{***}p < 0.001$, significantly different when compared with control group [Colour figure can be viewed at wileyonlinelibrary.com]

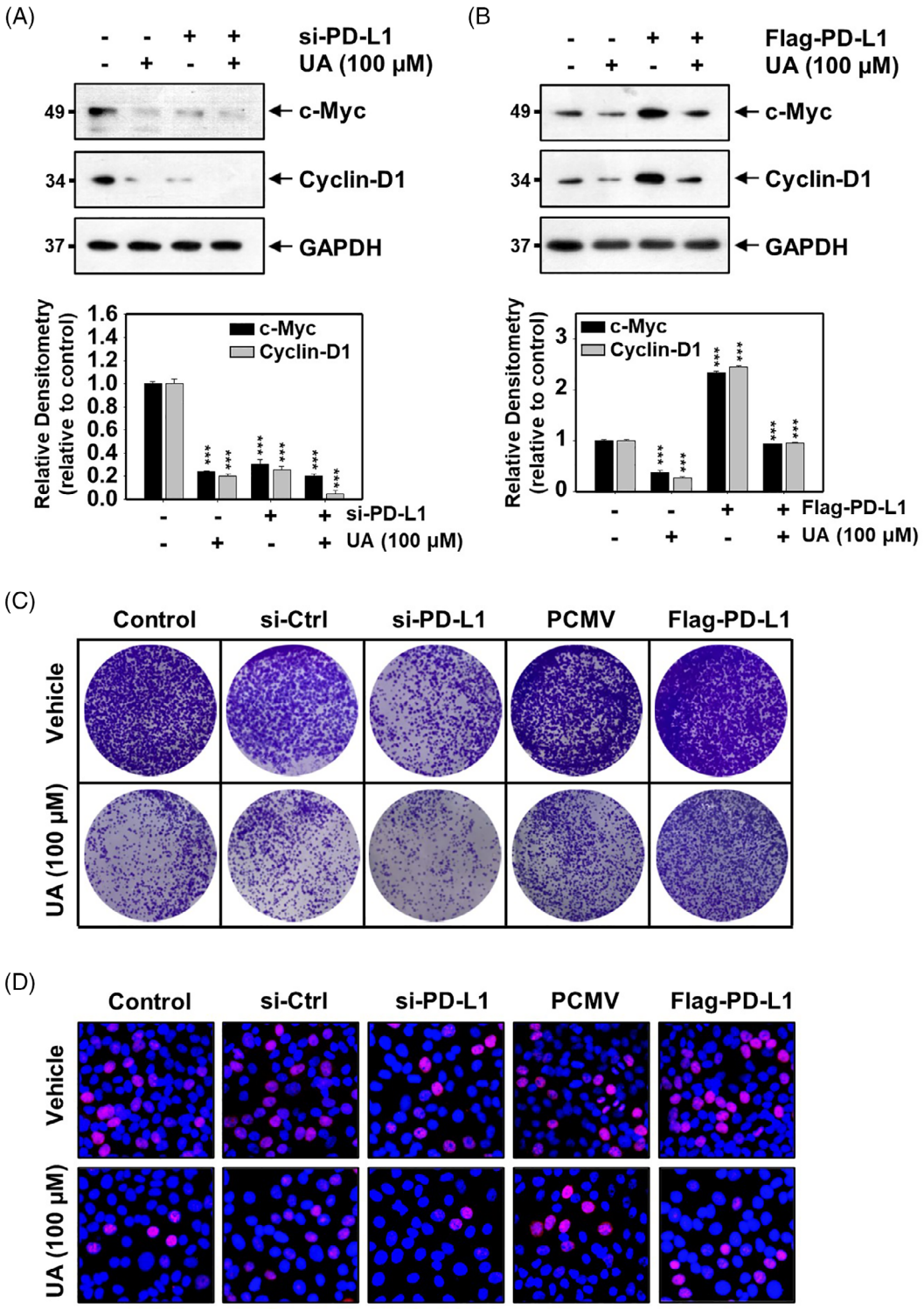

FIGURE 4 Effect of usnic acid on proliferation mediated by PD-L1 in human cervical cancer cells. (a and b) HeLa cells were transfected with PD-L1 siRNA or Flag-PD-L1. After 12 h, cells were treated with or without 100 μM usnic acid for 12 h. The expressions of c-Myc and Cyclin-D1 in HeLa cells were determined using western blotting. (c and d) HeLa cells were transfected with designated plasmids. Colony formation (c) and EdU experiment (d) detection of cells proliferation ability after usnic acid treatment for 12 h. All data are presented as the mean ± SD of three independent experiments and representative data are shown. ***$p < 0.001$ [Colour figure can be viewed at wileyonlinelibrary.com]

overexpressed in cells. Western blotting assay indicated that the expression of cell angiogenesis regulatory proteins, including VEGF and MMP-9 (Wang et al., 2015), was decreased by silencing of *CD274*, while this was enhanced by co-treatment with usnic acid (Figure 5a). VEGF and MMP-9 expression were promoted by over-expression of PD-L1; however, usnic acid treatment inhibited this

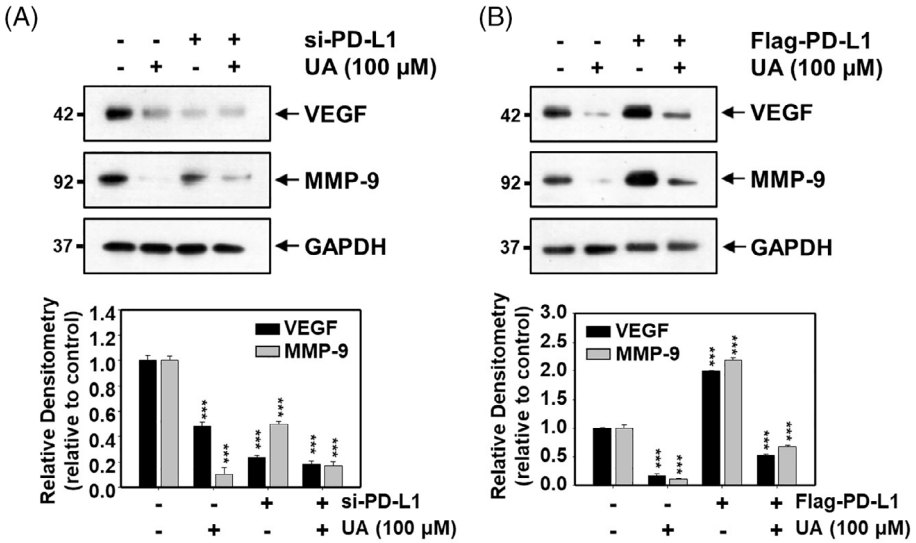

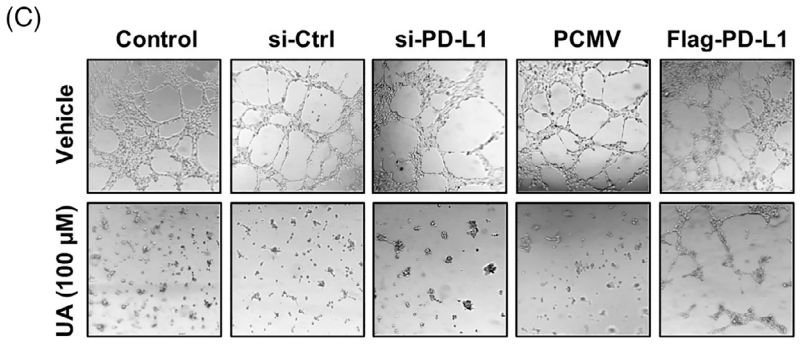

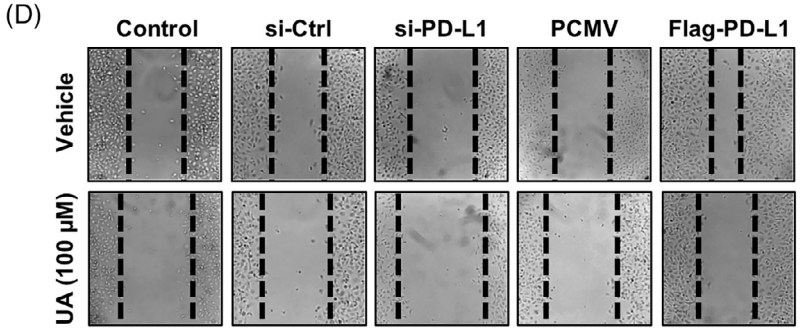

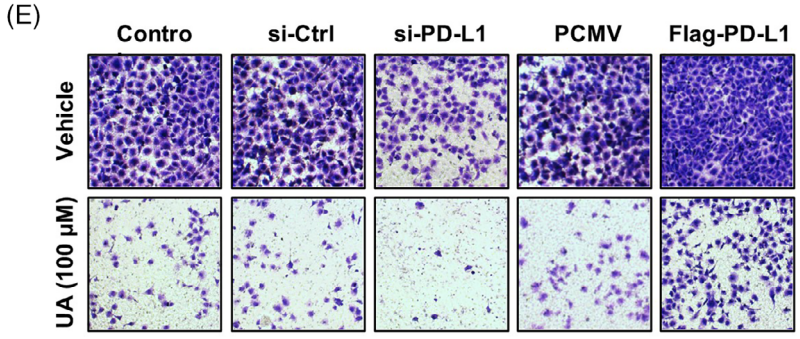

FIGURE 5 Effect of usnic acid on angiogenesis, migration, and invasion mediated by PD-L1 in endothelial cells. (a and b) After cells were transfected with PD-L1 siRNA or Flag-PD-L1, western blot detection of indicated proteins in HUVEC cells after treatment with usnic acid for 12 h. (c–e) HUVEC cells were transfected with designated plasmids. Tube formation assay (c), migration assay (d), and invasion assay (e) detection of cells angiogenesis ability after usnic acid treatment for 12 h. All data are presented as the mean ± SD of three independent experiments and representative data are shown. ***$p < 0.001$ [Colour figure can be viewed at wileyonlinelibrary.com]

increase (Figure 5b). The influence of usnic acid on antiangiogenic properties was further examined by tube formation, migration, and invasion assays. As displayed in Figure 5c, the number of complete network structures in HUVEC cells was greatly reduced by silencing of *CD274* or co-treatment with usnic acid. Overexpression of PD-L1 induced the formation of vascular structures; however, co-treatment

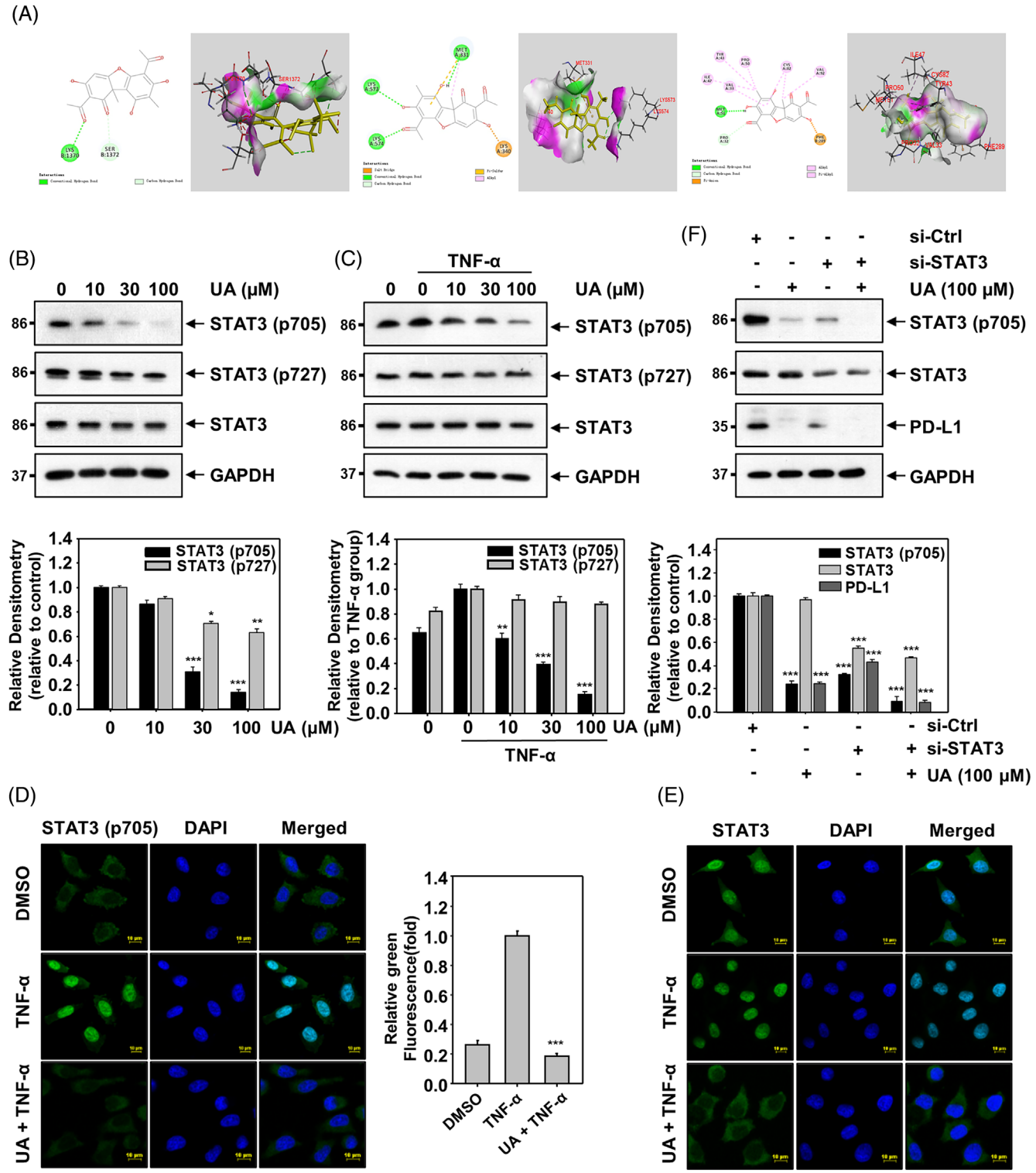

FIGURE 6 Effect of usnic acid on the PD-L1 expression mediated by STAT3 in HeLa cells. (a) Usnic acid was docked into the binding pocket of STAT3 (upper, PDB ID: 3CWG; middle, PDB ID: 4E68; lower, PDB ID: 5U5S). Binding structure was display in 2D (left) and 3D (right). The ligand is appeared in yellow. (b) HeLa cells were treated with the indicated concentrations of usnic acid for 12 h, pTyr705 STAT3, pSer727 STAT3, and STAT3 expressions were measured by western blot. (c) Under TNF-α-stimulated, HeLa cells were incubated with different concentrations of usnic acid for 12 h and cell lysates for proteins were analyzed by western blotting with indicated antibody. (d and e) Under TNF-α-stimulated, HeLa cells were incubated with or without 100 μM usnic acid for 12 h. Immunofluorescence (magnification, 400 ×) staining of the intracellular protein expression of pTyr705 STAT3 and STAT3 in HeLa cells. (f) HeLa cells were transfected with control or STAT3 siRNA. After 12 h, cells were treated with or without 100 μM usnic acid for 12 h. Whole-cell extracts were analyzed using western blotting with antibodies for pTyr705 STAT3, STAT3, and PD-L1. All data are presented as the mean ± SD of three independent experiments and representative data are shown. *$p < 0.05$, **$p < 0.01$, ***$p < 0.001$ [Colour figure can be viewed at wileyonlinelibrary.com]

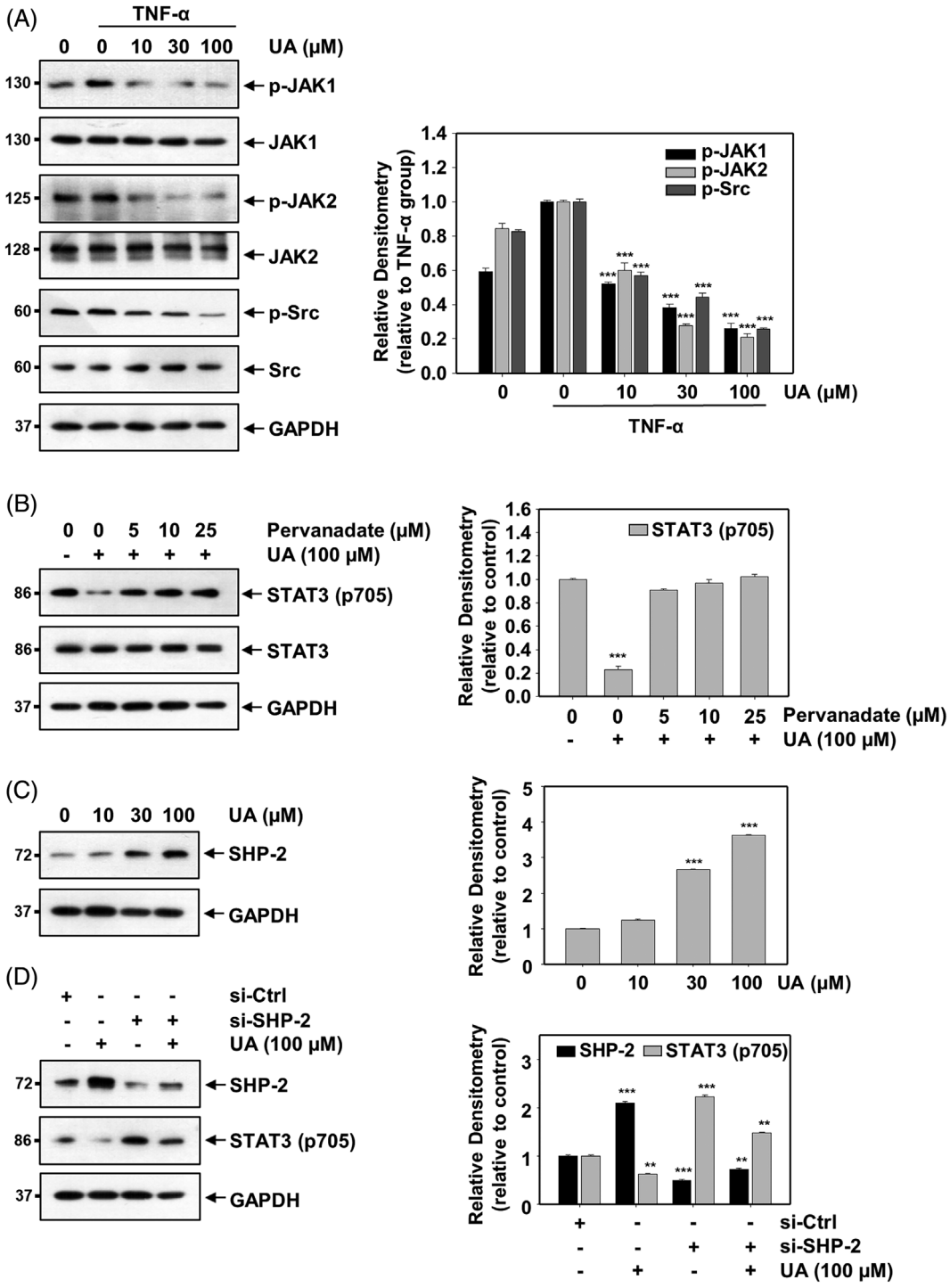

FIGURE 7 Effect of usnic acid on JAK1/JAK2 and Src signaling pathways. (a) HeLa cells were incubated under TNF-α-stimulated for 12 h, in the absence or presence of usnic acid (10 μM, 30 μM, and 100 μM). After 12 h incubation, phospho-JAK1, phospho-JAK2, and phospho-Src were detected using western blotting. (b) HeLa cells were treated with the indicated concentration of pervanadate and 100 μM usnic acid for 6 h, then pTyr705 STAT3 and STAT3 were detected by western blot analysis. (c) HeLa cells were treated with the indicated concentrations of usnic acid for 12 h, SHP-2 expression was measured by western blot. (d) HeLa cells were transfected with control or SHP-2 siRNA. After 12 h, cells were treated with or without 100 μM usnic acid for 12 h. Whole-cell extracts were analyzed using western blotting with antibodies for SHP-2 and pTyr705 STAT3. All data are presented as the mean ± SD of three independent experiments and representative data are shown. $^{**}p < 0.01$, $^{***}p < 0.001$

with usnic acid restrained this expression. These results were further confirmed by migration and invasion assays, whereby usnic acid suppressed the number of migrating and invading cells induced by PD-L1 (Figure 5d,e). Taken together, these findings suggest that usnic acid inhibits angiogenesis, migration, and invasion by decreasing PD-L1 in endothelial cells.

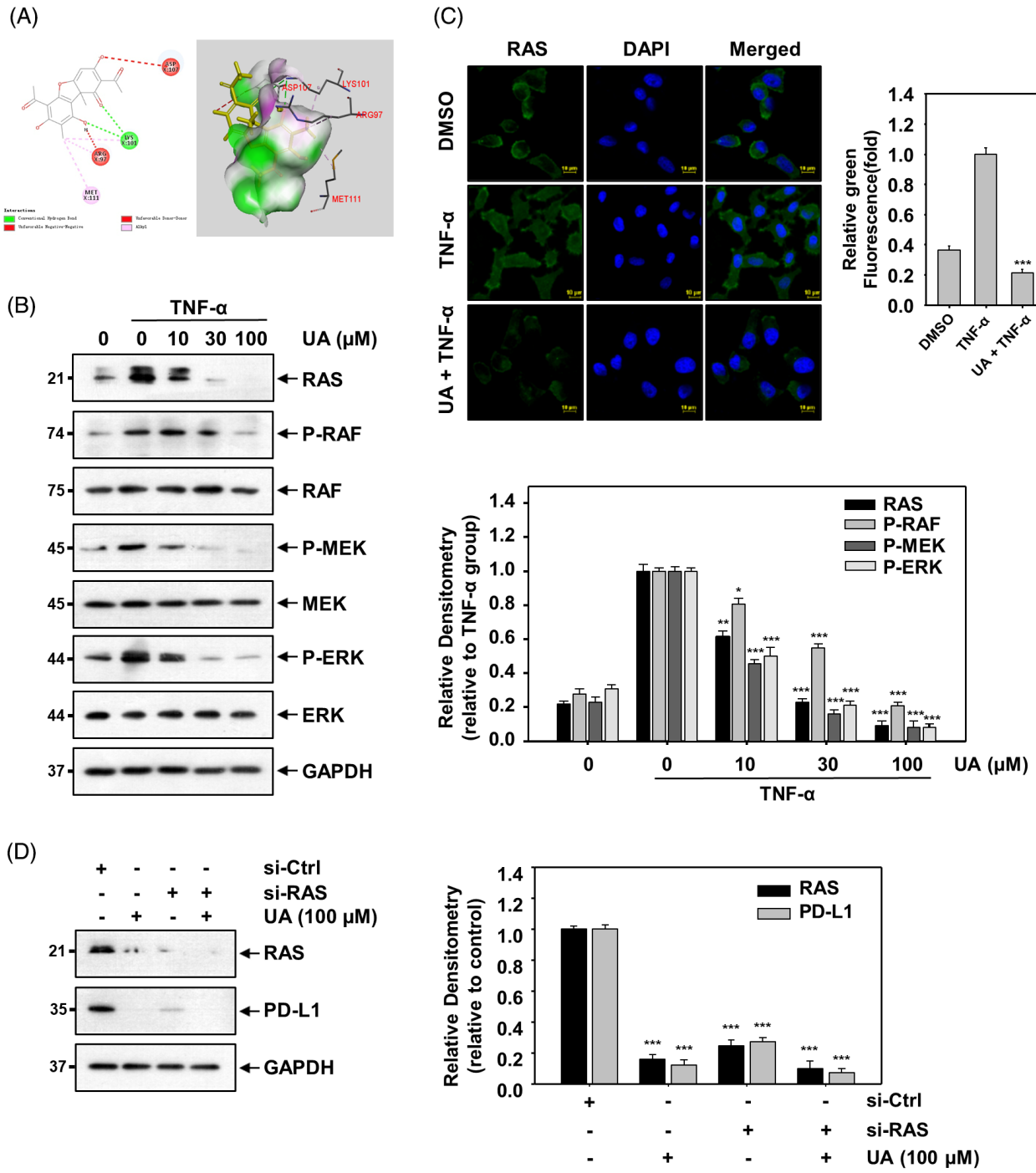

FIGURE 8 Effect of usnic acid on the PD-L1 expression mediated by RAS/RAF/MEK/ERK signaling pathways in HeLa cells. (a) (left, binding structure in 2D; right, binding structure in 3D) Usnic acid in the binding pocket of RAS (PDB ID: 2CL7). The ligand is appeared in yellow. (b) Under TNF-α-stimulated, HeLa cells were incubated with indicated concentrations of usnic acid for 12 h. The whole-cell lysates were analyzed using western blotting with indicated antibodies. (c) Under TNF-α-stimulated, HeLa cells were incubated with or without 100 μM usnic acid for 12 h. Immunofluorescence (magnification, 400 ×) staining of the intracellular protein expression of RAS in HeLa cells. (d) HeLa cells were transfected with control or RAS siRNA. After 12 h, cells were treated with or without 100 μM usnic acid for 12 h. Whole-cell extracts were analyzed using western blotting with antibodies for RAS and PD-L1. All data are presented as the mean ± SD of three independent experiments and representative data are shown. *$p < 0.05$, **$p < 0.01$, ***$p < 0.001$ [Colour figure can be viewed at wileyonlinelibrary.com]

3.7 | Usnic acid suppresses PD-L1 expression by inhibiting STAT3 in HeLa cells

The transcription of PD-L1 is regulated by continuous activation of STAT3 (Chen, Jiang, Jin, & Zhang, 2015). This study next investigated whether usnic acid can suppress PD-L1 expression by inhibiting STAT3 in HeLa cells. Molecular docking assays showed that usnic acid had a high-affinity interaction with protein 3CWG (binding pockets consisting of Lys1370 and Ser1372), protein 4E68 (binding pockets consisting of Met331, Lys340, Lys573, and Lys574), and protein

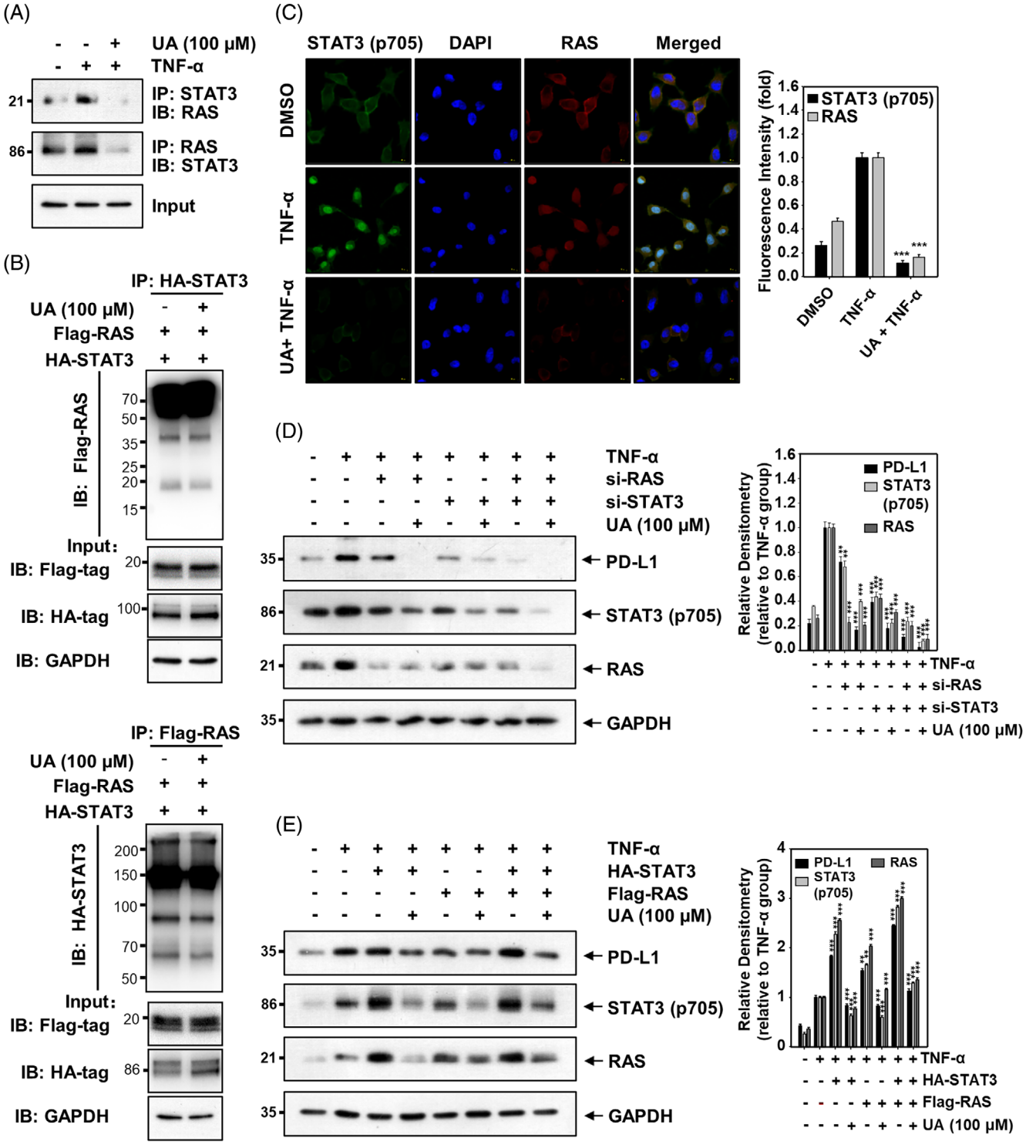

FIGURE 9 Effect of usnic acid on the PD-L1 expression mediated by the expression of pTyr705 STAT3 and RAS in HeLa cells. (a) HeLa cells were incubated under TNF-α-stimulated for 12 h in the absence or presence of 100 μM usnic acid. Immunoblot analysis of STAT3 and RAS proteins in cell lysates immunoprecipitated with indicated antibody. (b) HeLa cells were transfected with Flag-RAS and HA-STAT3 plasmids for 48 h. Before collection, cells were treated with 100 μM usnic acid for 12 h. Immunoblot analysis of STAT3 and RAS proteins in cell lysates immunoprecipitated with indicated antibody. (c) Under TNF-α-stimulated, HeLa cells were incubated with or without 100 μM usnic acid for 12 h. Immunofluorescence (magnification, 400 ×) staining of the intracellular protein expression of pTyr705 STAT3 and RAS in HeLa cells. (d) HeLa cells were transfected with designated siRNA plasmids for 48 h. Western blot detection of PD-L1, pTyr705 STAT3, and RAS in HeLa cells after treatment with usnic acid (100 μM) for 12 h under TNF-α-stimulated. (e) HeLa cells were transfected with HA-STAT3, Flag-RAS, or both for 48 h. Western blot detection of PD-L1, pTyr705 STAT3, and RAS in HeLa cells after treatment with usnic acid (100 μM) for 12 h under TNF-α-stimulated. All data are presented as the mean ± SD of three independent experiments and representative data are shown. $^{**}p < 0.01$, $^{***}p < 0.001$ [Colour figure can be viewed at wileyonlinelibrary.com]

5U5S (binding pockets consisting of Ile47, Cys82, Tyr43, Pro50, Met51, Val92, Pro32, Val33, and Phe289) of STAT3 (Figure 6a). Then, to examine whether usnic acid suppresses the phosphorylation and nuclear translocation of STAT3 in a dose-dependent manner, western blotting assays were performed. As shown in Figure 6b,c, in the absence or presence of TNF-α stimulation, usnic acid suppressed pTyr705 STAT3 in a concentration-dependent manner in HeLa cells, but did not significantly affect the expression of pSer727 STAT3 protein. Immunofluorescence assays showed that usnic acid completely inhibited the phosphorylation and nuclear translocation of STAT3 in HeLa cells (Figure 6d,e). Further research showed that the protein expression levels of pTyr705 STAT3, total STAT3, and PD-L1 were potently reduced in *STAT3*-knockdown HeLa cells (compare lane 1 with lane 3 in Figure 6f). Moreover, silencing of the *STAT3* gene and usnic acid treatment further reduced the protein expression of pTyr705 STAT3 and PD-L1 (compare lane 2 with lane 4 in Figure 6f). These results suggest that usnic acid attenuates PD-L1 expression by reducing pTyr705 STAT3 levels in the nucleus.

3.8 | Downregulation of the JAK1/JAK2 and Src signaling pathways by usnic acid correlates with inhibition of STAT3 expression

We next examined the effect of usnic acid on TNF-α-induced JAK1, JAK2, and Src activation in HeLa cells. As displayed in Figure 7a, usnic acid potently suppressed the TNF-α-induced phosphorylation of JAK1, JAK2, and Src in a concentration-dependent manner. To explore whether the inhibition of STAT3 upstream tyrosine kinases is because of the activation of protein tyrosine phosphatase (PTP), cells were treated with the indicated concentration of pervanadate, a tyrosine phosphatase inhibitor. Western blotting analysis revealed that sodium pervanadate reversed the usnic acid-induced inhibition of pTyr705 STAT3 in HeLa cells (Figure 7b). Activation of SHP-2 tyrosine phosphatase can negatively interfere with JAK/STAT3 signaling pathways (You, Yu, & Feng, 1999). Therefore, the effect of usnic acid on SHP-2 expression in HeLa cells was investigated. As shown in Figure 7c, usnic acid increased the protein expression of SHP-2 in a concentration-dependent manner. Further research showed that the protein expression levels of SHP-2 were potently reduced in SHP-2 (*PTPN11*)- knockdown HeLa cells (compare lane 1 with lane 3 in Figure 7d). Usnic acid-induced increases in SHP-2 expression were effectively inhibited in cells treated with PTPN11 siRNA (compare lane 2 with lane 4 in Figure 7d). These data indicated that SHP2 plays an important role in the suppression of STAT3 phosphorylation by usnic acid. Moreover, usnic acid inhibited pTyr705 STAT3 expression through JAK1/JAK2 and Src signaling pathways.

3.9 | Usnic acid inhibits PD-L1 expression by reducing RAS/RAF/MEK/ERK signaling pathways in HeLa cells

Mutations of *RAS* oncogene are prevalent in human malignancies and can upregulate PD-L1 expression (Sumimoto, Takano, Teramoto, & Daigo, 2016). To evaluate whether the depletion of RAS in usnic acid-treated HeLa cells modulates the expression of PD-L1, the following experiment was next carried out. Molecular docking assays showed that usnic acid bound to protein 2CL7 of the RAS binding pocket consisting of Asp107, Lys101, Arg97, and Met111 (Figure 8a). We next examined whether usnic acid suppresses RAS-related RAF/MEK/ERK pathway. The data demonstrated that usnic acid potently suppressed the expression of p-RAF, p-MEK, p-ERK, and RAS in a concentration-dependent manner under TNF-α treatment (Figure 8b). Immunofluorescence assay indicated that RAS expression was reduced in HeLa cells after usnic acid treatment under TNF-α stimulation (Figure 8c).

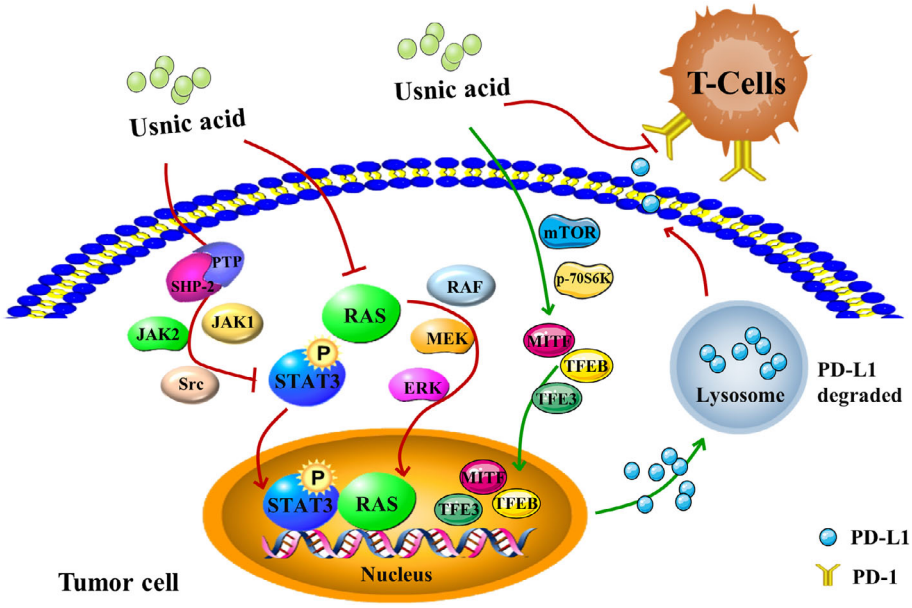

FIGURE 10 Scheme figure of proposed working model for usnic acid. Usnic acid inhibits PD-L1 protein synthesis by reducing STAT3 and RAS signaling pathways. Furthermore, usnic acid induces MiT/TFE nuclear translocation and promotes the translocation of PD-L1 to lysosomes for proteolysis. Usnic acid also inhibits PD-L1 expression on the cell surface and enhances the activity and killing capacity of T cells. In summary, usnic acid inhibits tumor proliferation by restrains PD-L1 expression [Colour figure can be viewed at wileyonlinelibrary.com]

Further research showed that protein expression levels of RAS and PD-L1 were potently reduced in *RAS* knockdown HeLa cells. Moreover, silencing of the *RAS* gene with usnic acid treatment further reduced the protein expression of RAS and PD-L1 (Figure 8d). Altogether, these findings indicated that usnic acid attenuated PD-L1 expression through inhibition of the RAS/RAF/MEK/ERK signaling pathways.

3.10 | Usnic acid inhibits PD-L1 expression by inhibiting STAT3 and RAS cooperatively

In addition, usnic acid exhibited inhibition pTyr705 STAT3, RAS, and PD-L1 expression in the other two cervical cancer cell lines (SiHa cells and CaSKi cells) (Supplementary Figure 5A and B), but exhibited the largest inhibitory effect on HeLa cells (Supplementary Figure 5C). To explore whether usnic acid suppresses the expression of PD-L1 by reducing STAT3 and RAS cooperatively, immunoprecipitation assays were performed. As shown in Figure 9a, the binding of STAT3 and RAS in HeLa cells was enhanced under TNF-α treatment. In addition, usnic acid inhibited the interaction of STAT3 and RAS. Consistently, this result was further confirmed in Figure 9b, the interaction of STAT3 and RAS was also blocked by usnic acid after cells were transfected with HA-STAT3 and Flag-RAS. Immunofluorescence assays indicated that the expression of pTyr705 STAT3 and RAS became downregulated in HeLa cells after usnic acid treatment under TNF-α stimulation (Figure 9c), while the protein expression levels of PD-L1 were markedly reduced in *STAT3* and *RAS* knockdown HeLa cells; this phenomenon was enhanced by usnic acid co-treatment (Figure 9d). Overexpression of STAT3 and RAS increased PD-L1 protein levels, which were inhibited by usnic acid co-treatment (Figure 9e). These results indicate that usnic acid can reduce PD-L1 protein levels by suppressing STAT3 and RAS cooperatively (Figure 10).

4 | DISCUSSION

Cancer immunotherapy is expected to prevent tumor recurrence and recreate the tumor microenvironment (Wang, Qin, & Zhao, 2015). Immune checkpoint inhibitors represented by the anti-PD-1/PD-L1 pathway have become a focus in new treatment approaches (Ke, Zhang, Xu, Zhao, & Dong, 2019). Immune checkpoint inhibitors can reverse the tumor immune microenvironment and enhance endogenous antitumor immune effects (Topalian, 2012). In addition, anti-PD-1 and anti-PD-L1 antibodies are being extensively studied because of their advantages of greater specificity, lower side effects, and better tumor control than others (Brahmer et al., 2012). Anti-PD-1/PD-L1 antibody monotherapy and combined radiation therapy have also shown good efficacy and few adverse reactions in antitumor clinical trials (Xu, Huang, Zheng, & Fan, 2018). According to literature, the PD-1/PD-L1 signaling pathway is closely related to the development of cervical cancer, and the emergence of immunotherapy has brought new hope for the treatment of human cervical cancer (Yang, Song, Lu, Sun, & Wang, 2013). In June 2018, pembrolizumab was approved by the Food and Drug Administration (FDA) for the treatment of advanced cervical cancer, with a response rate of 13.3–26.3% (Frenel, Tourneau, O'Neil, Ott, & Varga, 2017). Combination therapy with durvalumab PD-L1 antibody and tremelimumab CTLA-4 antibody has also entered the research phase of clinical trials for advanced cervical cancer (Gibney, Weiner, & Atkins, 2016). Therefore, blocking the PD-1/PD-L1 pathway is of great value for improving the survival of patients with cervical cancer.

In the present study, usnic acid was first identified as a potent PD-L1 inhibitor as it markedly inhibited PD-L1 expression, providing a powerful basis for it as an antitumor agent. PD-L1 was downregulated by usnic acid in a dose-dependent manner in human cervical cancer cells. In addition, usnic acid reduced the expression of PD-L1 on the surface of HeLa cells and increased the cytotoxicity of co-cultured T cells. Furthermore, the present study elucidated that the anti-tumor effect of usnic acid was through the STAT3 and RAS signal pathways cooperatively. Several studies have indicated that the activation of RAS caused a significant increase in PD-L1 mRNA expression in a time-dependent manner (Glorieux et al., 2020), and the depletion of STAT3 profoundly diminished PD-L1 expression on both the mRNA and protein levels (Marzec et al., 2008). In this article, usnic acid was shown to inhibit PD-L1 transcription. Consistent with previous studies, this inhibition may be partially implemented via suppression of the JAK-STAT3 and RAS/RAF/MEK/ERK pathways, which are closely involved in the activation of RAS and STAT3. However, it should be noted that the regulatory mechanisms of PD-L1 transcriptional expression are likely multifactorial processes, and it is worthy of further exploration. It has been shown that the persistent phosphorylation of STAT3 can promote PD-L1 expression and lead to tumorigenesis (Garcia et al., 2001; Luo et al., 2019). We observed that usnic acid inhibited STAT3 phosphorylation at Tyr705 by downregulating the JAK1/JAK2 and Src signaling pathways, and previous studies have indicated that SHP-2 also negatively regulates the JAK/STAT signaling pathway (Bard-Chapeau et al., 2011). In the current study, usnic acid induced SHP-2 protein expression. In addition, usnic acid inhibited Tyr705 STAT3 was reversed by pervanadate, indicating the main function of this PTP in STAT3 dephosphorylation. We noted that usnic acid downregulated STAT3 phosphorylation was associated with the induction of SHP-2 protein expression.

The RAS/RAF/ERK signaling cascade is a major regulatory pathway downstream of EGFR (Ritt, Abreu-Blanco, Bindu, Durrant, & Morrison, 2016). It is involved in various physiological and pathological processes, including cell proliferation, differentiation, and malignant transformation, and plays an important role in tumor development (Kennedy, Morton, Manoharan, Nelson, & Adams, 2011). We showed that usnic acid downregulated RAS protein synthesis through the RAF/MEK/ERK pathways. There are complex interactions between the JAK/STAT3 and RAS/ERK signaling pathways that are related to cancer development. Our data revealed that usnic acid inhibited the interaction of STAT3 and RAS and downregulated PD-L1 protein synthesis by reducing STAT3 and RAS cooperatively. Up to now, there are no reports about anti-cervical cancer

drugs simultaneous with strong inhibitory effects on PD-1/PD-L1, JAK/STAT3, and RAS/RAF/ERK pathways. Moreover, we did not set a positive control in our experimental design. Therefore, it is of great significance to develop novel anti-cervical cancer based on the above pathways.

Proteasomal or lysosomal pathways can promote PD-L1 protein degradation (Wang et al., 2019). Lysosomes are organelles that break down biological macromolecules such as proteins, nucleic acids, and polysaccharides (Settembre, Fraldi, Medina, & Ballabio, 2013), and lysosomal dysfunction causes the proliferation and invasion of cancer cells. LysoTracker staining results confirmed that PD-L1 was colocalized with LAMP1 (lysosome marker) and usnic acid promoted translocation of PD-L1 to the acid lysosomes for proteolysis, which is consistent with the previous report that the YWHL-containing signal peptide in PD-L1 directed its localization in lysosomes (Chen, 2004). A recent study demonstrated that huntingtin-interacting protein 1–related (HIP1R) binds to PD-L1 by its conserved C-terminal domain and targets PD-L1 to lysosomal degradation by HIP1R (966–979) containing an intrinsic lysosomal sorting signal (Wang et al., 2019). Whether HIP1R is regulated by usnic acid and involved in lysosomal degradation of PD-L1 requires further investigations.

The MiT/TFE family is a major regulator of autophagy, which can increase the number of lysosomes and transport proteins into the lysosome for degradation. The nuclear translocation of MITF, TFE3, and TFEB can induce the expression of lysosomal catabolic function (Slade & Pulinilkunnil, 2017). MTORC1 directly phosphorylates MiT/TFE proteins and retains them in the cytoplasm (Martina & Puertollano, 2013). Our study demonstrated that usnic acid activated lysosome biogenesis in HeLa cells. Usnic acid induced MiT/TFE nuclear translocation through the suppression of mTOR/p70S6K pathways, and promoted lysosomal catabolic activity for PD-L1 degradation. Our results are in agreement with recent reports that the inactivation of mTOR and p70S6K (a well-recognized mTORC1 substrate that can be used as a reporter of mTORC1 activity) promotes MITF/TFE3/TFEB nuclear translocation (Wang et al., 2020). Previous studies showed that the cellular localization of mTOR and the activity of mTORC1 can be regulated by raptor or Rag GTPases, the effector in Ragulator-Rag-mTORC1 complex (Sancak et al., 2010). Whether usnic acid could affect mTORC1 by regulating raptor or Rag GTPases requires further investigation.

High expression of PD-L1 is an important factor in tumor formation, development, and metastasis, and enhances the ability of cancer cells to resist the immune system (Chen et al., 2015). The main functions of c-Myc and cyclin D1 are respectively to promote cell division and proliferation. Our data revealed that the expressions of c-Myc and cyclin-D1 were decreased by silencing of PD-L1, which downregulated cell proliferation; this effect was enhanced by co-treatment with usnic acid. Usnic acid was also found to inhibit angiogenesis and cell migration and invasion by inhibiting the expression of angiogenesis regulatory proteins, including VEGF and MMP-9. However, it should be pointed out that we only carry out the tests on a cell model (HeLa), and the impact on other cervical cancer cell lines is worthy of further exploration.

In summary, these findings indicated that usnic acid inhibited PD-L1 protein synthesis by reducing STAT3 and RAS signaling pathways cooperatively. Furthermore, usnic acid induced MiT/TFE nuclear translocation through the suppression of mTOR signaling pathway and promoted the translocation of PD-L1 to lysosomes for proteolysis. Usnic acid inhibited PD-L1 expression on the cell surface and enhanced the activity and killing capacity of T cells, thereby inhibiting tumor proliferation, angiogenesis, migration, and invasion. Taken together, usnic acid should be considered as a potential novel lead compound for the exploitation of an anti-cervical cancer drug, and our study provides novel insights for the development of usnic acid related drugs.

ACKNOWLEDGEMENTS

This work was partially supported by National Natural Science Foundation of China, No. 81660608 and 81760657. This work was partially supported by the 111 Project of the base of recruiting talents for disciplinary innovation on natural resources & functional molecules. This work was partially supported by the 13th five-year program of science and technology of the ministry of education of Jilin province (JJKH20191152KJ).

AUTHOR CONTRIBUTIONS

Xuejun Jin and Juan Ma conceived and designed the study. Tong Xin Sun and Ming Yue Li performed all the experiments and wrote. Zhi Hong Zhang, Jing Ying Wang, Yue Xing, and MyongHak Ri prepared all the figures. Cheng Hua Jin, Guang Hua Xu, Lian Xun Piao, Hong Lan Jin, Hong Xiang Zuo, Juan Ma, and Xuejun Jin reviewed and edited the manuscript. All authors read and approved the manuscript.

CONFLICT OF INTERESTS

The authors declare that there are no financial conflict of interests in regard to this work.

DATA AVAILABILITY STATEMENT

The data that support the findings of this study are available from the corresponding author upon reasonable request.

ORCID

Xuejun Jin https://orcid.org/0000-0001-6998-2602

REFERENCES

Aoki, Y., Niihori, T., Narumi, Y., Kure, S., & Matsubara, Y. (2008). The RAS/-MAPK syndromes: Novel roles of the RAS pathway in human genetic disorders. *Human Mutation*, *29*(8), 992–1006.

Arbyn, M., Weiderpass, E., Bruni, L., de Sanjosé, S., Saraiya, M., Ferlay, J., & Bray, F. (2020). Estimates of incidence and mortality of cervical cancer in 2018: A worldwide analysis. *Lancet Global Health*, *8*(2), e191–e203.

Badoual, C., Hans, S., Merillon, N., Van Ryswick, C., Ravel, P., Benhamouda, N., … Besnier, N. (2013). PD-1–expressing tumor-infiltrating T cells are a favorable prognostic biomarker in HPV-associated head and neck cancer. *Cancer Research*, *73*(1), 128–138.

Baek, S. H., Lee, J. H., Ko, J. H., Lee, H., Nam, D., Lee, S. G., … Ahn, K. S. (2016). Ginkgetin blocks constitutive STAT3 activation and induces

apoptosis through induction of SHP-1 and PTEN tyrosine phosphatases. *Phytotherapy Research*, *30*(4), 567–576.

Bard-Chapeau, E. A., Li, S., Ding, J., Zhang, S. S., Zhu, H. H., Princen, F., … Poli, V. (2011). Ptpn11/Shp2 acts as a tumor suppressor in hepatocellular carcinogenesis. *Cancer Cell*, *19*(5), 629–639.

Brahmer, J. R., Tykodi, S. S., Chow, L. Q., Hwu, W.-J., Topalian, S. L., Hwu, P., … Odunsi, K. (2012). Safety and activity of anti–PD-L1 antibody in patients with advanced cancer. *New England Journal of Medicine*, *366*(26), 2455–2465.

Burr, M. L., Sparbier, C. E., Chan, Y.-C., Williamson, J. C., Woods, K., Beavis, P. A., … Dawson, M. A. (2017). CMTM6 maintains the expression of PD-L1 and regulates anti-tumour immunity. *Nature*, *549*(7670), 101–105.

Chai, E. Z. P., Shanmugam, M. K., Arfuso, F., Dharmarajan, A., Wang, C., Kumar, A. P., … Goh, B. C. (2016). Targeting transcription factor STAT3 for cancer prevention and therapy. *Pharmacology & Therapeutics*, *162*, 86–97.

Chang, M. Y. (1998). *Kang Ai Zhong Yao* (pp. 291–293). Hunan Province: Hunan Science and Technology Press.

Chen, J., Jiang, C. C., Jin, L., & Zhang, X. D. (2015). Regulation of PD-L1: A novel role of pro-survival signalling in cancer. *Annals of Oncology*, *27* (3), 409–416.

Chen, L. (2004). Co-inhibitory molecules of the B7-CD28 family in the control of T-cell immunity. *Nature Reviews Immunology*, *4*(5), 336–347.

Cheng, J. H., & Li, Y. B. (1998). *Kang Ai Zhi Wu Yao Ji Qi Yan Fang* (pp. 422–423). Jiangxi Province: Jiangxi Science and Technology Press.

Coelho, M. A., de Carné Trécesson, S., Rana, S., Zecchin, D., Moore, C., Molina-Arcas, M., … Barnouin, K. (2017). Oncogenic RAS signaling promotes tumor immunoresistance by stabilizing PD-L1 mRNA. *Immunity*, *47*(6), 1083, e1086–1099.

De Simone, V., Franze, E., Ronchetti, G., Colantoni, A., Fantini, M., Di Fusco, D., … Pallone, F. (2015). Th17-type cytokines, IL-6 and TNF-α synergistically activate STAT3 and NF-kB to promote colorectal cancer cell growth. *Oncogene*, *34*(27), 3493–3503.

Drosten, M., Dhawahir, A., Sum, E. Y., Urosevic, J., Lechuga, C. G., Esteban, L. M., … Barbacid, M. (2010). Genetic analysis of Ras signalling pathways in cell proliferation, migration and survival. *EMBO Journal*, *29*(6), 1091–1104.

Frenel, J. S., Tourneau, C. L., O'Neil, B., Ott, P. A., & Varga, A. (2017). Safety and efficacy of Pembrolizumab in advanced, programmed death ligand 1-positive cervical cancer: Results from the phase Ib KEYNOTE-028 trial. *Journal of Clinical Oncology*, *35*(36), 4035–4041.

Garcia, R., Bowman, T. L., Niu, G., Yu, H., Minton, S., Muro-Cacho, C. A., … Parsons, S. (2001). Constitutive activation of Stat3 by the Src and JAK tyrosine kinases participates in growth regulation of human breast carcinoma cells. *Oncogene*, *20*(20), 2499–2513.

Gibney, G. T., Weiner, L. M., & Atkins, M. B. (2016). Predictive biomarkers for checkpoint inhibitor-based immunotherapy. *Lancet Oncology*, *17* (12), e542–e551.

Glorieux, C., Xia, X., He, Y. Q., Hu, Y., Cremer, K., Robert, A., … Huang, P. (2020). Regulation of PD-L1 expression in K-ras-driven cancers through ROS-mediated FGFR1 signaling. *Redox Biology*, *38*, 101780.

Haigis, K. M., Kendall, K. R., Wang, Y., Cheung, A., Haigis, M. C., Glickman, J. N., … Shannon, K. M. (2008). Differential effects of oncogenic K-Ras and N-Ras on proliferation, differentiation and tumor progression in the colon. *Nature Genetics*, *40*(5), 600.

Ingólfsdóttir, K. (2002). Usnic acid. *Phytochemistry*, *61*(7), 729–736.

Ju, X., Zhang, H., Zhou, Z., Chen, M., & Wang, Q. (2020). Tumor-associated macrophages induce PD-L1 expression in gastric cancer cells through IL-6 and TNF-α signaling. *Experimental Cell Research*, *396*(2), 112315.

Juneja, V. R., McGuire, K. A., Manguso, R. T., LaFleur, M. W., Collins, N., Haining, W. N., … Sharpe, A. H. (2017). PD-L1 on tumor cells is sufficient for immune evasion in immunogenic tumors and inhibits CD8 T cell cytotoxicity. *Journal of Experimental Medicine*, *214*(4), 895–904.

Ke, M., Zhang, Z., Xu, B., Zhao, S., & Dong, J. (2019). Baicalein and baicalin promote antitumor immunity by suppressing PD-L1 expression in hepatocellular carcinoma cells. *International Immunopharmacology*, *75*, 105824.

Kennedy, A. L., Morton, J. P., Manoharan, I., Nelson, D. M., & Adams, P. D. (2011). Activation of the PIK3CA/AKT pathway suppresses senescence induced by an activated RAS oncogene to promote tumorigenesis. *Molecular Cell*, *42*(1), 36–49.

Kim, K. H., Park, Y. J., Jang, H. J., Lee, S. J., Lee, S., Yun, B. S., & Lee, S. W. (2020). Rugosic acid A, derived from *Rosa rugosa* Thunb., is novel inhibitory agent for NF-κB and IL-6/STAT3 axis in acute lung injury model. *Phytotherapy Research*, *34*(12), 3200–3210.

Kim, K. J., Jeong, M. H., Lee, Y., Hwang, S. J., Shin, H. B., Hur, J. S., & Son, Y. J. (2018). Effect of usnic acid on osteoclastogenic activity. *Journal of Clinical Medicine*, *7*(10), 345.

Kumar, R. V., & Bhasker, S. (2013). Potential opportunities to reduce cervical cancer by addressing risk factors other than HPV. *Journal of Gynecologic Oncology*, *24*(4), 295–297.

Lee, J. C., Sim, D. Y., Lee, H. J., Im, E., Choi, J. B., Park, J. E., … Jung, J. H. (2020). MicroRNA216b mediated downregulation of HSP27/STAT3/AKT signaling is critically involved in lambertianic acid induced apoptosis in human cervical cancers. *Phytotherapy Research*, *35*, 898–907.

Li, M. Y., Zhang, Z. H., Wang, Z., Zuo, H. X., & Jin, X. (2019). Convallatoxin protects against dextran sulfate sodium-induced experimental colitis in mice by inhibiting NF-κB signaling through activation of PPARγ. *Pharmacological Research*, *147*, 104355.

Li, Y., Xu, M., Ding, X., Yan, C., Song, Z., Chen, L., … Yang, C. (2016). Protein kinase C controls lysosome biogenesis independently of mTORC1. *Nature Cell Biology*, *18*(10), 1065–1077.

Li, Z., Zhu, Y. T., Xiang, M., Qiu, J. L., & Lin, F. (2020). Enhanced lysosomal function is critical for paclitaxel resistance in cancer cells: Reversed by artesunate. *Acta Pharmacologica Sinica*, *42*, 1–9.

Liontos, M., Kyriazoglou, A., Dimitriadis, I., Dimopoulos, M.-A., & Bamias, A. (2019). Systemic therapy in cervical cancer: 30 years in review. *Critical Reviews in Oncology/Hematology*, *137*, 9–17.

Liu, Y., Wu, L., Tong, R., Yang, F., Yin, L., Li, M., … Lu, Y. (2019). PD-1/PD-L1 inhibitors in cervical cancer. *Frontiers in Pharmacology*, *10*, 65.

Luo, F., Luo, M., Rong, Q.-X., Zhang, H., Chen, Z., Wang, F., … Fu, L.-W. (2019). Niclosamide, an antihelmintic drug, enhances efficacy of PD-1/PD-L1 immune checkpoint blockade in non-small cell lung cancer. *Journal for Immunotherapy of Cancer*, *7*(1), 1–13.

Luzina, O. A., & Salakhutdinov, N. F. (2018). Usnic acid and its derivatives for pharmaceutical use: A patent review (2000-2017). *Expert Opinion on Therapeutic Patents*, *28*(6), 477–491.

Ma, J., Li, J., Wang, K. S., Mi, C., Piao, L. X., Xu, G. H., … Jin, X. (2016). Perillyl alcohol efficiently scavenges activity of cellular ROS and inhibits the translational expression of hypoxia-inducible factor-1α via mTOR/4E-BP1 signaling pathways. *International Immunopharmacology*, *39*, 1–9.

Martina, J. A., & Puertollano, R. (2013). Rag GTPases mediate amino acid–dependent recruitment of TFEB and MITF to lysosomes. *Journal of Cell Biology*, *200*(4), 475–491.

Marzec, M., Zhang, Q., Goradia, A., Raghunath, P. N., Liu, X., Paessler, M., … Wasik, M. A. (2008). Oncogenic kinase NPM/ALK induces through STAT3 expression of immunosuppressive protein CD274 (PD-L1, B7-H1). *Proceedings of the National Academy of Sciences of the United States of America*, *105*(52), 20852–20857.

Mora, N., Rosales, R., & Rosales, C. (2007). R-Ras promotes metastasis of cervical cancer epithelial cells. *Cancer Immunology, Immunotherapy*, *56* (4), 535–544.

Perera, R. M., & Zoncu, R. (2016). The lysosome as a regulatory hub. *Annual Review of Cell & Developmental Biology*, *32*(1), 223.

Ritt, D. A., Abreu-Blanco, M. T., Bindu, L., Durrant, D. E., & Morrison, D. K. (2016). Inhibition of Ras/Raf/MEK/ERK pathway signaling by a stress-induced phospho-regulatory circuit. *Molecular Cell*, *64*(5), 875.

Sancak, Y., Bar-Peled, L., Zoncu, R., Markhard, A. L., Nada, S., & Sabatini, D. M. (2010). Ragulator-Rag complex targets mTORC1 to the lysosomal surface and is necessary for its activation by amino acids. *Cell*, *141*(2), 290–303.

Sandri, M. (2016). Protein breakdown in cancer cachexia. *Seminars in Cell and Developmental Biology*, *54*, 11–19.

Settembre, C., Fraldi, A., Medina, D. L., & Ballabio, A. (2013). Signals from the lysosome: A control centre for cellular clearance and energy metabolism. *Nature Reviews Molecular Cell Biology*, *14*(5), 283–296.

Shukla, S., Shishodia, G., Mahata, S., Hedau, S., Pandey, A., Bhambhani, S., … Bharti, A. C. (2010). Aberrant expression and constitutive activation of STAT3 in cervical carcinogenesis: Implications in high-risk human papillomavirus infection. *Molecular Cancer*, *9*, 282.

Slade, L., & Pulinilkunnil, T. (2017). The MiTF/TFE family of transcription factors: Master regulators of organelle signaling, metabolism and stress adaptation. *Molecular Cancer Research*, *15*(12), 1637–1643.

Sumimoto, H., Takano, A., Teramoto, K., & Daigo, Y. (2016). RAS–mitogen-activated protein kinase signal is required for enhanced PD-L1 expression in human lung cancers. *PLoS One*, *11*(11), e0166626.

Tong, L., Li, J., Li, Q., Wang, X., Medikonda, R., Zhao, T., … Yang, X. (2020). ACT001 reduces the expression of PD-L1 by inhibiting the phosphorylation of STAT3 in glioblastoma. *Theranostics*, *10*(13), 5943–5956.

Topalian, S. L. (2012). Safety, activity, and immune correlates of anti-PD-1 antibody in cancer. *New England Journal of Medicine*, *366*(26), 2443–2454.

Wang, F., Ma, J., Wang, K. S., Mi, C., Lee, J. J., & Jin, X. (2015). Blockade of TNF-α-induced NF-κB signaling pathway and anti-cancer therapeutic response of dihydrotanshinone I. *International Immunopharmacology*, *28*(1), 764–772.

Wang, H., Yao, H., Li, C., Shi, H., Lan, J., Li, Z., … Xu, J. (2019). HIP1R targets PD-L1 to lysosomal degradation to alter T cell-mediated cytotoxicity. *Nature Chemical Biology*, *15*(1), 42–50.

Wang, M., Wang, H., Tao, Z., Xia, Q., Hao, Z., Prehn, J. H. M., … Ying, Z. (2020). C9orf72 associates with inactive rag GTPases and regulates mTORC1-mediated autophagosomal and lysosomal biogenesis. *Aging Cell*, *19*(4), e13126.

Wang, W. J., Qin, S. H., & Zhao, L. (2015). Docetaxel enhances CD3+ CD56+ cytokine-induced killer cells-mediated killing through inducing tumor cells phenotype modulation. *Biomedicine & Pharmacotherapy*, *69*, 18–23.

Wang, Y., Wang, H., Yao, H., Li, C., & Xu, J. (2018). Regulation of PD-L1: Emerging routes for targeting tumor immune evasion. *Frontiers in Pharmacology*, *9*, 536.

Xu, X., Huang, Z., Zheng, L., & Fan, Y. (2018). The efficacy and safety of anti-PD-1/PD-L 1 antibodies combined with chemotherapy or CTLA 4 antibody as a first-line treatment for advanced lung cancer. *International Journal of Cancer*, *142*(11), 2344–2354.

Yang, W., Song, Y., Lu, Y. L., Sun, J. Z., & Wang, H. W. (2013). Increased expression of programmed death (PD)-1 and its ligand PD-L1 correlates with impaired cell-mediated immunity in high-risk human papillomavirus-related cervical intraepithelial neoplasia. *Immunology*, *139*(4), 513–522.

You, M., Yu, D. H., & Feng, G. S. (1999). Shp-2 tyrosine phosphatase functions as a negative regulator of the interferon-stimulated Jak/STAT pathway. *Molecular and Cellular Biology*, *19*(3), 2416–2424.

Zammataro, L., Lopez, S., Bellone, S., Pettinella, F., Bonazzoli, E., Perrone, E., … Han, C. (2019). Whole-exome sequencing of cervical carcinomas identifies activating ERBB2 and PIK3CA mutations as targets for combination therapy. *Proceedings of the National Academy of Sciences*, *116*(45), 22730–22736.

Zhang, H. H., Kuang, S., Wang, Y., Sun, X. X., & Gu, Y. (2015). Bigelovin inhibits STAT3 signaling by inactivating JAK2 and induces apoptosis in human cancer cells. *Acta Pharmacologica Sinica*, *36*, 507–516.

SUPPORTING INFORMATION

Additional supporting information may be found online in the Supporting Information section at the end of this article.

How to cite this article: Sun TX, Li MY, Zhang ZH, et al. Usnic acid suppresses cervical cancer cell proliferation by inhibiting PD-L1 expression and enhancing T-lymphocyte tumor-killing activity. *Phytotherapy Research*. 2021;35:3916–3935. https://doi.org/10.1002/ptr.7103